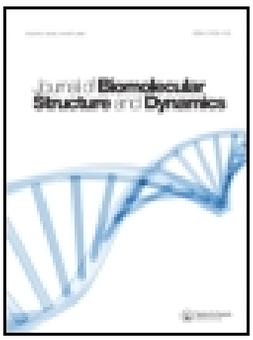

Taylor & Francis
Taylor & Francis Group

Journal of Biomolecular Structure and Dynamics

ISSN: 0739-1102 (Print) 1538-0254 (Online) Journal homepage: http://www.tandfonline.com/loi/tbsd20

Structural Analysis and Molecular Docking of Trypanocidal Aryloxy-quinones in Trypanothione and Glutathione Reductases: A Comparison with Biochemical Data

Brenda Vera, Karina Vázquez, Carolina Mascayano, Ricardo A. Tapia, Victoria Espinosa, Jorge Soto-Delgado, Cristian O. Salas & Margot Paulino

To cite this article: Brenda Vera, Karina Vázquez, Carolina Mascayano, Ricardo A. Tapia, Victoria Espinosa, Jorge Soto-Delgado, Cristian O. Salas & Margot Paulino (2016): Structural Analysis and Molecular Docking of Trypanocidal Aryloxy-quinones in Trypanothione and Glutathione Reductases: A Comparison with Biochemical Data, Journal of Biomolecular Structure and Dynamics

To link to this article: http://dx.doi.org/10.1080/07391102.2016.1195283

Accepted author version posted online: 27 May 2016.
Published online: 27 May 2016.

Publisher: Taylor & Francis

Journal: *Journal of Biomolecular Structure and Dynamics*

DOI: http://dx.doi.org/10.1080/07391102.2016.1195283

Structural Analysis and Molecular Docking of Trypanocidal Aryloxy-quinones in Trypanothione and Glutathione Reductases: A Comparison with Biochemical Data

Brenda Vera[a], Karina Vázquez[b,c], Carolina Mascayano[d], Ricardo A. Tapia[b], Victoria Espinosa[e], Jorge Soto-Delgado[f], Cristian O. Salas[b*] and Margot Paulino[a*]

[a] Centro de Bioinformática estructural, DETEMA, Facultad de Química, UdelaR, Montevideo, Uruguay; [b] Facultad de Química, Pontificia Universidad Católica de Chile, Santiago, Chile; [c] Campus de Ciencias Agropecuarias, Facultad de Medicina Veterinaria y Zootecnia, Universidad Autónoma de Nuevo León, México; [d] Departamento de Ciencias del Ambiente, Facultad de Química y Biología, Universidad de Santiago, Chile, Santiago, Chile; [e] Centro de investigaciones biomédicas y aplicadas, Escuela de Medicina, Facultad de Ciencias Médicas, Universidad de Santiago, Chile, Santiago, Chile; [f] Departamento de Ciencias Químicas, Facultad de Ciencias Exactas, Universidad, Andrés Bello, Quillota 980, Viña del Mar, Chile.

* Corresponding authors. Emails: *margot@fq.edu.uy*; *cosalas@uc.cl*

Running Title: Aryloxy-quinones in Trypanothione and Glutathione Reductases: *In vitro* and *in silico* studies.

Keywords: Molecular docking; aryloxy-quinones; trypanothione reductase; glutathione reductase; Chagas disease.

Abstract

A set of aryloxy-quinones, previously synthesized and evaluated against *Trypanosoma cruzi* epimastigotes cultures were found more potent and selective than nifurtimox. One of the possible mechanisms of the trypanocidal activity of these quinones could be inhibition of trypanothione reductase (TR). Considering that glutathione reductase (GR) is the equivalent of TR in humans, biochemical, kinetic and molecular docking studies in TR and GR were envisaged and compared with the trypanocidal and cytotoxic data of a set of aryloxy-quinones.

Biochemical assays indicated that three naphthoquinones (**Nq-h**, **g** and **d**) selectively inhibit TR and the TR kinetic analyses indicated that **Nq-h** inhibit TR in a non-competitive mechanism.

Molecular docking were performed in TR and GR in three putative binding sites: the catalytic site, the dimer interface and the NADPH binding site.

In TR and GR, the aryloxy-quinones were found to exhibit high affinity for a site near it cognate binding site in a place in which the non-competitive kinetics could be justified.

Taking as examples the three compounds with TR specificity (**Nq-h**, **Nq-g** and **Nq-d**) the presence of a network of contacts with the quinonic ring sustained by the triad of Lys62, Met400´, Ser464' residues, seems to contribute hardly to the TR specificity.

Compound **Nq-b**, a naphthoquinone with nitrophenoxy substituent, proved to be the best scaffold for the design of trypanocidal compounds with low toxicity. However, the compound displayed only a poor and

non-selective effect towards TR indicating that TR inhibition is not the main reason for the antiparasitic activity of the aryloxy-quinones.

Abbreviations:

TS_2 : bis(gamma-glutamyl-cysteinyl-glycinyl)spermidine; RGS: 4-*N*-malonyl cysteinyl-2,4-diaminobutyrate disulfide; DMSO: Dimethyl sulfoxide; ROS: Reactive oxygen species; TR: Trypanothione reductase; GR: Glutathione reductase; MMFF94x: Merck Molecular Force Field; PLIF: Protein-ligand interaction fingerprints; PDB: Protein data bank; MOE: Molecular operating environment; ps: Picosecond; FAD: Flavin adenine dinucleotide; NADPH: Nicotinamide adenine dinucleotide phosphate; RMS: Root Mean Square

1. Introduction

Parasitic diseases are a major obstacle to human health and economic development in many parts of the world, and cause high rates of mortality and morbidity (WHO 2011). Current therapies against these diseases are unsatisfactory, with treatment failure being common due to widespread resistance and severe side effects (Viotti et al. 2006; Bern et al. 2007; Yun et al. 2009; Rassi, Rassi Jr. & Marin-Neto 2010; Bern 2011). Thus, there is a need for the development of new, efficient and safe drug (Manoel-Caetano Fda & Silva 2007; Woodcock & Woosley 2008; Molina et al. 2014; Hoelz et al., 2015; (Carraro, Iribarne, & Paulino, 2016). In recent years, naphthoquinones and heterocyclic derivatives are considered privileged structures in the development of novel drugs against parasitic diseases such as trypanosomiasis (Salas, Faundez, Morello, Maya & Tapia 2011; Prati et al. 2015).

There are several proposed mechanisms of action for the trypanocidal activity of quinone derivatives. One of them is the well-known ability of quinones for generating reactive oxygen species (ROS) through redox cycling with molecular oxygen and consequently oxidative stress and cell death (O'Brien 1991; Henry & Wallace 1996; Kovacic 2007; Paulino et al. 2008; Benites et al. 2010).

The metabolic differences between the parasite and host cells to avoid the damage mediated by ROS are considerable (Gutteridge & Halliwell 2000; Salas et al. 2011). Trypanothione reductase (TR) constitutes a major component of the general oxidative-stress defense in *T. cruzi* (Turrens 2004) and is absent in mammals. The main function of TR is to maintain a reducing intracellular environment by keeping

trypanothione in the dithiol state (Gonzalez-Chavez, Olin-Sandoval, Rodiguez-Zavala, Moreno-Sanchez & Saavedra 2015). TR is essential in all trypanosomatids. Parasites with lowered TR activity display an increased sensitivity towards hydrogen peroxide (Fairlamb, Blackburn, Ulrich, Chait & Cerami 1985; Gonzalez-Chavez et al. 2015). The counterpart of the parasite TR in the mammalian host is glutathione reductase (GR). A comparison with the available crystal structures of GR (Pai & Schulz 1983; Karplus & Schulz 1987; Pai, Karplus & Schulz 1988; Karplus & Schulz 1989; Berkholz, Faber, Savvides & Karplus 2008) reveals that the overall structure of the two enzymes is highly conserved. There is an overall 40 % sequence identify and both enzymes are homodimers. TR may also replace thioredoxin reductase, although trypanosomatids do possess a conventional thioredoxin.

The key feature of TR and GR is the mutually exclusive specificity for their cognate disulfide substrate. Thus, in principle, it should be possible to inhibit selectively the parasite enzyme without affecting the mammalian one. A detailed analysis of the enzymes (Iribarne, Paulino, Aguilera, Murphy & Tapia 2002) indicates that in both TR and GR several alternative sites exist in addition to the binding sites for the disulfide substrate and NADPH as well as the dimer interface.

For a set of aryloxy-quinones previously synthetized and tested for their trypanocidal and cytotoxic activities (Vazquez et al. 2015), it was proposed that their selective antiparasitic activities may correlate with the inhibition of TR. To prove this hypothesis, here we report on the biochemical and kinetic analysis of recombinant *T. cruzi* TR and human GR inhibition. In parallel, *in silico* molecular docking studies of TR/GR complexes with aryloxy-quinones in all putative binding sites aimed at a deeper understanding of the atomic interactions between these compounds and TR and GR, respectively. As a result, quinone derivatives with good and selective TR inhibitor capacity and with low GR affinity can be proposed as candidates to develop more effective drugs against Chagas and other diseases caused by trypanosomatids.

2. Methodology

A set of 28 aryloxy-quinones (Figure 1) were previously synthetized and tested (Vazquez et al. 2015). The set of quinones was divided in three sub-sets based on three main scaffolds as naphthoquinones, quinolinequinones and furanoquinones. Moreover, each main scaffold has different aryloxy substituents. To understand the manner in which these molecules function in the parasite, as well as in the couple TR/GR trypanosomatids and mammalian enzymes, in a first step of this work twenty of these molecules

were selected to make TR/GR inhibition and kinetics studies. In a second step an *in silico,* strategy was applied to the entire set of quinones.

2.1 Biochemical studies

TcTR was prepared following a published procedure (Walsh, Bradley & Nadeau 1991). Trypanothione disulfide (TS_2) was generated enzymatically as described previously (Comini, Dirdjaja, Kaschel & Krauth-Siegel 2009).

2.1.1 Trypanothione reductase assays

The activity of TR was measured in 40 mM Hepes, 1mM EDTA, pH 7.5 at 25 °C. The assay mixture contained, in a total volume of 1 mL, 100 μM NADPH, 5-10 mU of TcTR and 50 μL DMSO as control or the same volume with the tested compound dissolved at a final concentration of 100 μM when the quinone inhibition was tested. The reaction was started by addition of 100 μM of TS_2 and NADPH consumption was measured by following the absorbance decrease at 340 nm at 25 °C ($\varepsilon = 6.22\ mM^{-1}\ cm^{-1}$) (Persch et al. 2014). From these data, the percentage of inhibition was calculated. Many compounds proved to be insoluble under the assay conditions and thus could only be measured at rather low concentrations. One representative compound of each sub-set of compounds (**Nq-h**, **Fq-c** and **Qq-b**) was subjected to a detailed kinetic analysis.

2.1.2 Glutathione reductase assays

Glutathione reductase was purified from human erythrocytes by the method previously reported (Worthington & Rosemeyer, 1974). The enzyme was stored at a concentration of 5 mg/ml in potassium phosphate buffer, pH 7.0, I 0.1 M, containing 0.2 M KCI, 1 mM EDTA and 0.1 % (v/v) 2-mercaptoethanol.

The activity of human GR was measured in 200 mM KCl, 60 mM K_2HPO_4 and 1mM EDTA, pH 6.9 at 25°C. The assay mixture contained in a total volume of 1 ml, 100 μM NADPH and 5–20 mU of hGR and 5 mM of inhibitor on DMSO.

After checking for non-specific NADPH oxidation for two minutes, 1.1 mM of GSSG was added to start the enzymatic reaction. The decrease in NADPH concentration was monitored spectrophotometrically. Residual enzyme activity in the presence of inhibitor was determined relative to controls containing

DMSO according to Nordhoff et al. (Nordhoff, Bucheler, Werner & Schirmer 1993; Maran, Fernandez, Barbieri, Font & Ruiz 2009; Fernandez-Blanco, Font & Ruiz 2016).

2.2 *In Silico* assays

All calculations were done running the Molecular Operating Environment (MOE 2015.10, Chemical Computing Group Inc., http://www.chemcomp.com) suite on Linux, on a workstation with a quad-core processor Hyperthread equipped.

A molecular docking of 28 carbo and heterocyclic derivatives of aryloxy-quinones was done to study the interactions with the putative enzymatic receptors TR and GR. This procedure implies a ligand and a receptor preparation, the development of a validated docking procedure and the molecular docking itself.

2.2.1 Ligand preparation: Modelling and conformational analysis

The three-dimensional structures of the 28 molecules under study (Vazquez et al. 2015) (Figure 1) were submitted to energy minimization by means of MMFF94x force field (Halgren 1996) and the program suite MOE. To use all flexibility capacity of the program, a conformational analysis was performed for all naphthoquinones, quinolinequinones and furanoquinones using the low-mode molecular dynamics (LowModeMD) approach (Labute 2010) to search minimum energy conformers. The resulting conformations are saved to the output database provided they meet the energetic and geometric criteria.

An energy minimization was done and terminated when the Root Mean Square (RMS) gradient test fall below 0.005 kcal/mol. The maximum number of energy minimization iterations was selected as 500. Two conformations are judged equal if the optimal heavy atom RMS superposition distance is less than the specified tolerance of 0.25 Å. All conformations with an energy greater than the sum of the global minimum energy plus a cutoff of 7 kcal/mol were discarded.

2.2.2 Crystal structure of the putative targets

Trypanothione reductase

The catalytic function of TR is the reduction of its cognate substrate trypanothione disulfide (TS2) to the dithiol form $T(SH)_2$. TR is active as a homodimer with a subunit mass of about 52 kD. The two identical catalytic sites are composed of residues of both subunits and comprise at least two regions, namely the NADPH site and the disulfide substrate site, which are separated by the flavin ring (Paulino et al. 2005).

The crystal structure of *T. cruzi* TR complexed with its physiological substrate TS2 was obtained from the Protein Data Base (PDB 1BZL), 2.4Å resolution (Bond et al. 1999). The homodimeric protein is composed of two peptide chains each containing 486 amino acids, two molecules of the cofactor flavin adenine dinucleotide (FAD) and two molecules of ligand, the *bis*(gamma-glutamyl-cysteinyl-glycinyl)spermidine (TS_2). Both TR co-crystallized ligands are posed each one in both catalytic sites.

Glutathione reductase

The crystal structure of human glutathione reductase was obtained from the PDB base (4GR1) with 2.4Å resolution (Janes & Schulz 1990). GR is a homodimer with two chains of 478 amino acids and a molecule of the cofactor flavin adenine dinucleotide (FAD) each. It is cocrystallized with a molecule of 4-N-malonyl cysteinyl-2,4-diaminobutyrate disulfide (RGS).

2.2.3 Quinones putative binding sites

To identify possible quinones-binding sites in the crystal structures of GR and TR was used the Site Finder module of the MOE 2015.10. Forty four putative sites in TR and fifty five in GR were detected. The Site Finder shows the findings as red (polar) or grey (apolar) spheres and a number that is the total count of spheres represents the size of a site. The sites have been analyzed in their size as well their structure and amino acid composition. The greater detected sites in both enzymes were the catalytic sites described above in the crystallographic structures. The Site Finder detected too the NADPH binding sites in both enzymes. Finally, for both enzymes, a site localized in the interface surface between both monomers conforming the dimer was identified (Figure 2). Several crystal structures of GR-inhibitor complexes have shown binding of the ligands at this cavity (e.g. Bilzer et al. 1984; Savvides & Karplus 1996).

2.2.3.1 Catalytic binding site and neighborhoods

Cys53 and Cys58 form the catalytic redox-active site dithiol/disulfide of TR and are located at the bottom of the cleft near the isoalloxazine ring of FAD (Bond et al. 1999). In GR, the respective residues are Cys58 and Cys63 (Pai & Schulz, 1983; Pai, Karplus & Schulz, 1988; Karplus, Pai & Schulz, 1989; Janes & Schulz 1990).

When the trypanothione disulfide binding site in TR is described based on a list of contacting amino acids at a 4.5Å distance of TS_2, it could observed that amino acids from both A and B chains participate in the binding (Bond et al. 1999).

Research from our groups gave detailed information about these structural characteristics. (Hikichi, Paulino, Hansz & Tapia 1995; Iribarne et al. 2002; Paulino et al. 2005; Iribarne, Paulino, Aguilera & Tapia 2009).

The overall structure of the active site of GR is similar to that of TR. However, in contrast to the negatively charged TS_2 binding site in TR, the GSSG binding site in GR displays an overall positive charge.

A hydrophobic region named "Z-site" was defined in 1991 by el-Waer (el-Waer, Douglas, Smith & Fairlamb 1991). They suggested the Z-site as a relevant binding pocket for TR inhibitors although Glu466 and Glu467, the residues mainly responsible for the electrostatic interactions with the inhibitors, are conserved in GR and TR (de Paula da Silva, Bernardes, da Silva, Zani, & Carvalho, 2012). Thus, it is difficult to assume a specific binding of TR inhibitors at this site. Indeed, although docking simulations yielded the Z-site as favored binding site, the crystal structure revealed the inhibitor at the hydrophobic wall lining the TS2 binding site (Persch et al. 2014). Here we will demonstrate that for aryloxy-quinones, a mixture of both catalytic and Z-site residues, in its neighborhood, could confer selectivity.

2.2.3.2 Alternative putative binding sites

In each active site of the homodimer, the cofactor FAD is found, together with the dithiol/disulfide bridge, essential for catalysis. During catalysis, reducing equivalents flow from NADPH to the disulfide substrate (e.g.; trypanothione) with FAD and the disulfide bridge as intermediates. Two proton relays, one at each site, modulate the transfer. This complexity justifies the proposal of the NADPH site as a putative binding site, in the same way by which the endogenous substrate binding site was proposed before.

At the subunit interface, both enzymes have a cavity that was marked in the Site Finder strategy, as a likely binding site. This is in accordance with previous crystal structures of GR inhibitor complexes showing ligand binding at this site (e.g. Bilzer et al. 1984, Savvides & Karplus 1996). In comparison to

GR, the cavity of TR is more extended and narrow, contacting both catalytic sites in neighborhood of the above described Z-site (Figure 2). This topology like a bridge between both catalytic sites caused us to think that this site may bind molecules. For this reason, in the docking approaches we compared this region with other sites.

2.2.4 Molecular docking

Separate configurational databases in which each one of naphthoquinones, quinolinequinones and furanoquinones configurations were used. As ligand it was used a configurational database of molecules.

Four sites are assayed separately. The catalytic binding sites were defined from a 4.5 Å sphere around the co-crystallized ligand of TR and GR respectively. The interface site definition was made through the Site Finder procedure above described. In the case of NADPH, a 4.5 Å sphere around the FAD adenine moiety defined the site.

Docking validation tests were performed with three set of conformational databases for naphthoquinones, quinolinequinones and furanoquinones and the Catalytic Site 1. Two placement methods: Triangle Matcher and Alpha PMI (Udatha, Sugaya, Olsson & Panagiotou 2012) were assayed. Affinity dG (AdG) (Halgren 1996) and London dG were assayed for scoring and re-scoring. Finally, MMFF94x force field was used to energy minimize the resulting structures.

2.2.5 Protein Ligand Interaction Fingerprints (PLIF)

The PLIF (protein−ligand interaction fingerprints) descriptors implemented in the MOE were used as a benchmark with respect to interaction fingerprints. Interactions are classified as hydrogen bonds, ionic interactions, and surface contacts according to the residues. The PLIF descriptors for all protein-bound ligands were generated with the default parameter set in MOE and presented in Population Display and the Barcode display.

The Population Display is a histogram showing the number of ligands (Y-axis) with which each residue (plotted in the X-axis) interacts. In the Barcode representation of binding interactions, they are horizontal lines (rows) that correspond to each of the studied compounds.

Additionally, two other analysis of PLIF results were performed and PLIF-ContactMap and PLIF-HeatMap were generated.

2.2.6 H-Bond Ligand Interactions

The Ligand Interactions application provides a tool to visualize an active site of a complex in diagrammatic form. A selection of interacting entities, which includes hydrogen-bonded residues, close but non-bonded residues, solvent molecules and ions are drawn about the ligand, their positions in 2D being chosen to be representative of the observed 3D distances, as well as taking into account aesthetic considerations.

3. Results and Discussion

3.1 Enzymatic inhibition and kinetics

3.1.1. TR and GR inhibition screening

Table 1 summarizes the experimental data obtained for all aryloxy-quinones investigated in in this study. The trypanocidal activity towards *T. cruzi*, cytotoxicity versus J-774 cells (Vazquez et al. 2015), as well as the *in vitro* TR/GR inhibitor activities are given.

Considering the three subsets of aryloxy-quinones studied, a naphthoquinone (**Nq-h**) proved to be the most active inhibitor of TR. However, no correlation between TR inhibition and the antiparasitic activity efficiency was observed. Whereas compound **Nq-b** showed the highest trypanocidal activity, it was a comparably weak inhibitor of TR and was even more active against GR. Thus, the compound is a good example that other mechanisms are responsible for the cellular mode of action of the quinones.

Nq-b is a naphthoquinone with a nitro substituent in its aryloxy moiety which may be the reason for its excellent trypanocidal activity (IC_{50} *T. cruzi* epimastigote = 0.02 μM). It is even more potent than nifurtimox (IC_{50} *T. cruzi* epimastigote = 7 μM) and possibly acts by a similar mechanism.

Nq-h was the most effective and selective inhibitor of TR. Its trypanocidal activity was good; although ten-fold lower than that of **Nq-b**. The halogen (Br) on the naphthoquinone and the O-naphthyl substituent suggest that the electronegativity as well as the planar aromaticity may confer selectivity for TR versus GR inhibition.

3.1.2. TR kinetic assays

Nq-h, **Qq-b** and **Fq-c** were selected as representatives for the naphthoquinone, quinolinquinone and furanquinone subsets and subjected to a detailed kinetic analysis. The type of inhibition was derived from Lineweaver-Burk plots (Supplementary Material Figure I). The inhibitor constants Ki were calculated from direct plots. The data obtained are shown in Table 2. All three compounds inhibited TR with a non-competitive type of inhibition indicating that their binding site does not coincide with that for TS_2. With a *Ki*–value of 1.1 μM, **Nq-h** was clearly the best TR inhibitor.

3.2 The 3D structure of the assayed quinones database and it Structure-Activity Relationships (SAR)

Table 3 summarizes the main structural characteristics and results to allow a SAR analysis of the trypanocidal and TR inhibitory activities.

3.2.1 SAR with respect to the trypanocidal activity

Being that the aim of this search for a trypanocidal non-toxic drug is to improve the design of nifurtimox (better growth inhibition together with a lesser toxicity), it was been considered that a quinone with a good trypanocidal activity must inhibit *T. cruzi* growth in a concentration under 0.17 μM, a medium activity will correspond to concentrations between 0.17 and 7 μM, and quinones with inhibitory concentrations over 7 μM (that of nifurtimox) will be considered with low activity.

As we concluded in a previous paper (Vazquez et al 2015), when comparing the naphthoquinones, furanoquinones and quinolinequinones, the naphthoquinone moiety proved to be the best substructure for trypanocidal activity as well as lower toxicity. This is because the naphthoquinones were specially analyzed here. Inside the naphthoquinone sample, we could observe many variants including the addition of nitro, bromine, phenyl or naphthyl moieties.

The presence of two putative redox active moieties: the quinonic ring and the nitro-phenyloxy group (**Nq-b**) is an example of a very good improvement giving to the molecule very good (the best) activity in *T. cruzi*. With respect to the toxicity (J-774 cells), a comparison with nifurtimox seems put in evidence that the presence of the quinonic planar structure together with a phenoxy group, gave to the molecule selectivity in favor to the parasite inhibition (low toxicity than nifurtimox). Finally, the addition of a halogen when a nitro moiety is present (like in **Nq-e**) seems to lower the *T. cruzi* selective growth inhibition.

The presence of a halogen or a dimethyl-phenyloxy (comparing **Nq-a** with **Nq-d** or **Nq-a** with **Nq-c**) did not helped to improve the *T. cruzi* growth inhibition either to lower the toxicity.

The results of molecules with an alpha or beta naphtyloxy moieties, with or without a bromine atom in the structure, seems indicate that in which refers the *T. cruzi* growth inhibition these moieties have quite similar impact. In some cases (comparing **Nq-i** with **Nq-j**) the bromination contributes to lower the toxicity when a beta naphthyloxy is present in the structure. The halogenation of an alpha naphtyloxy moiety as in the case of the **Nq-h** seems not to give to the molecule a special either selective activity (compared with **Nq-g**).

3.2.2 SAR with respect to the TR/GR inhibitory activity

The nitro moiety, so good in the design of a trypanocidal molecule, is not related with a good and selective TR inhibition. This is the case of **Nq-b** and **Nq-e**, which are not selective TR inhibitors even if they are non-toxic and trypanocidal molecules.

A naphthoquinone scaffold accompanied by a phenyl nitro compound like that of **Nq-b** is depicted as the ideal scaffold to reach higher *T. cruzi* inhibition together with very low toxicity, even if the action mechanism will not be the selective inhibition of TR.

The phenoxy group is good when it has a bromination in the naphthyl moiety (**Nq-d**).

The alpha naphthyloxy group as in **Nq-h** and **Nq-g,** seems to be related to a selective TR inhibition. When the alpha naphthyloxy group has an halogen (**Nq-h**) the selectivity is as good than when it is absent (**Nq-g**).

They are no TR inhibition data to analyse the influence of a beta naphthyl (as it is the case of **Nq-j** of **Nq-i**) even if both have low activity in GR.

In the last columns of the Table 3, main questions referring these observations were YES/NO answered. In consequence, those molecules with both YES answers (*T. cruzi* and TR selective inhibition): **Nq-h, d** and **g,** were selected to further discussion.

Nq-h, **d** and **g,** are good and selective *T. cruzi* inhibitors and at the same time of TR. For these three cases, the hypothesis of a selective inhibition of TR associated to a good and selective inhibition of *T. cruzi* growth is true. Considering that the **Nq-h** was the best, we could say that for the set of studied

aryloxy-quinones, a naphthoquinone moiety, accompanied with an alpha naphthyloxy substituent is the scaffold to lead the design of a trypanocidal, non-toxic and TR selective inhibitor drug.

3.3 Molecular docking

The previous observations were limited by the lacking of all necessary experimental results. This is because in this work we had the proposal of doing all *in silico* evaluation of the complete set of the quinones under study. The *in silico* will be in this case, complementary to all the discussion envisaged in the Section 3.2.

3.3.1 Docking validation

The validation step aimed into obtaining the broader range of energies to assure a good conformation sampling. The full set of ten naphthoquinones, nine quinolinequinones and nine furanquinones was used to generate three conformational databases of 63, 59 and 64 conformers respectively and they were docked in the Catalytic Site 1 of the TR (1BZL).

The results are presented in the Table 4. The best results were obtained for the Alpha PMI and the London G methods.

As the second criterion of validation, we look for a maximum overlap between the cocrystallyzed and docked TS_2. The Alpha PMI and the London G methods were used to dock the TS_2 in the catalytic Site 1. The overlapping between the cocrystallyzed and docked TS_2 was measured and resulted an RMSD (Root Mean Square Deviation) of 2.02Å.

In consequence, the procedure was declared validated.

3.3.2 Docking in the catalytic sites of TR and GR

The three conformational databases were used as “ligand” in the docking.

As "Receptor" they were settled all atoms of TR or GR. As "Site", it was defined a sphere of 4.5Å around the crystallographic ligand TS_2 or RGS respectively. After selection, TS_2 (or RGS) molecules were deleted and FAD atoms remained as unselected atoms.

With the aim of comparing with in the experimental results shown in the Table 1, in the Supplementary Material Table A were detailed the ΔG of the best docked conformation for each set of aryloxy-quinones. All poses were classified in two ranges of high and low energies. All high energetic poses

were red colored ant the other in yellow. The result are shown in the Figure 2 and in Supplementary Material Figures II and III.

As it could be observed inside the left bottom frame of the Figure 2A, two populations of naphthoquinones are detected in TR. The red colored poses, that is, the more energetic bindings, are in a site in the borderline between the Z site and the catalytic site.

When the furane and quinoline quinones were docked against the catalytic site 1 of TR, similar results were obtained being the more energetic bindings near to the catalytic site in the borderline with the Z site (Supplementary Material Figures IIa and IIIa).

To describe graphically this new aryloxy-quinones site, an electrostatic map was obtained for TR and GR (Figures 2A and 2B left top frames). The Electrostatic Feature Map in MOE is an application of the Poisson-Boltzmann Equation (PBE) to the prediction of electrostatically preferred locations of hydrophobic, H-bond acceptor and H-bond donor locations.

The best energies in the docking against GR were observed in a subsite of the catalytic site 1 similar to that detected for TR (left bottom frame in Figure 2B and Supplementary Material Figures IIb and IIIb).

3.3.3 Docking in the alternative sites of TR and GR

The docking for the three conformational databases in the interface site of TR (1BZL) and y GR (4GR1) shown that all best scored poses were placed in the middle of the interface but with lesser free energies than in the other assayed sites (data not shown). As an example, in the Supplementary Material Figures IV are shown the naphthoquinones docked in the interface site of TR and GR.

The results of the docking in the NADPH sites in TR and GR, are shown in the Supplementary Material Table A and Figure V for the case of naphthoquinones.

3.4 Analysis of docked complexes in TR and GR

3.4.1 Analysis of docking in the catalytic site by Protein Ligand Interaction Fingerprints (PLIF)

A massive analysis of contacts between docked quinones in TR and GR was performed by means of Protein Ligand Interaction Fingerprints (PLIF). For data visualization, the Barcode and Population Display as well as PLIF-ContactMap and PLIF-HeatMap tools were used.

All Side chain H-donor or acceptor (ChDon/ChAcc), Backbone H-donor or acceptor (BkDon/BkAcc), Solvent H-donor and acceptor (O), Ionic attraction (I) and Surface contact (Surf) were analyzed.

3.4.1.1 Barcode and Population Display. The Figures 3a and 3b shown the Barcode Display and Figures 4a and 4b shown the Population Display (or histogram) made for all 28 docked quinones in GR and TR respectively.

Two list of contacts emerges and they are, in the case of TR is: Lys62, Thr66, Leu399´, Met400', His401', Lys402', Asp432', Asn433, His461', Thr463´ and Ser464'.

In the case or GR the list of contacts is: Lys67, Asn71, Tyr106, Ile113, Tyr114, Ile343, Arg347, Thr404', Met406', Leu438', His467', Thr469´, Ser470', Glu473' and Thr476'.

Those contacts that have counterpart in TR/GR are highlighted in bold: Lys62´in TR is Lys67 in GR; Thr66 in TR is Asn71 in GR; Leu399´in TR is Met406´in GR (a non-conservative change); His461´in TR is the His467´in GR; Thr463´in TR is Thr469´in GR and Ser464´in TR is Ser470´in GR.

All other contacts of docked quinones in TR doesn´t have a counterpart in GR and vice versa.

In the Figures 4a and 4b, the Y-axis shows the relative counts for the bits, directly related with the number of contacts. For example, the **Lys62** has the three higher bars and that means that this amino acid makes three kind of contacts with the most of quinones. On the contrary, Asn433 has three bars with very low Y-value meaning that it forms three different and non-frequent contacts.

Lys62 is of most importance for the TR binding and is evidenced by the three columns in the Figure 3a. In the case of GR, Lys67 forms hydrogen bonds with all the analyzed quinones evidenced by the two columns if the Figure 3b. Even if the mammalian enzyme offers a more electrostatic region to binding and that the Lys62 is conserved in GR, some selectivity for TR could be evidenced by an increased number of contacts.

Leu399´in TR is a contact detected for quinones that is a non conserved residue in GR (Met406´). This contact seems to be important to the pose of quinones in the TR. However, Met406´makes more contacts in GR than Leu399´in TR, allowing to conclude that both residues are of similar important in the TR or GR binding.

The **Met400'** in TR appears, as a surface contact in the PLIF analysis for **Nq-h**, **Qq-d** and **Fq-b** and it is absent as contact in GR. For this reason, we could propose this contact as important for the TR

specificity. This residue deserved special consideration in the interaction analysis of quinones by Molfetta et al (de Molfetta, de Freitas, da Silva & Montanari 2009).

Referring the contact with **Ser464'** in TR (Ser470' in GR), it appears more frequently in TR than in GR as an important H-bonding interaction in the PLIF analysis.

In GR (Figure 4b), there is a differential contact found in the **Glu473**' (not present in TR) giving to this environment the electrostatic differential characteristic pointing to a selective binding in favor of TR.

3.4.1.2 PLIF-ContactMap and PLIF-HeatMap.

The PLIF-ContactMap and the PLIF-HeatMap were created from the PLIF analysis as an *ad hoc* designed tool to observe all docked conformations by means of a colorful image of binding in TR and GR that confirmed and completed the previous observations. They are presented in the Table 5 and in the Supplementary Material Table B.

In the case of PLIF-ContactMap, to each given contact it was assigned a number representing the percentage of conformers of a quinone making a contact with a given amino acid in TR or GR. For data visualization, the numbers of contacts were highlighted by means of a color gradient from dark red (100%) to light blue (4%). The result is shown in the Table 5 (PLIF-ContactMap). Alternatively, the percentage of contacts was associated to the intensity of the color from dark to light red (PLIF-HeatMap).

Lys62 in TR make two kind of H-bond acceptor and surface contacts with high percentage of conformations making contacts (e.g. 64% for **Nq-h**). **Met400´** has unique and colorful annotations in TR representing the contacts made by a high percentage of quinones conformations (e.g. 55% for **Nq-h**). Finally, higher percentage of conformations make four kind of contacts (two H-bond side chain acceptor and two backbone H-bond acceptor) with **Ser 464´** in TR (e.g. 69% for **Nq-d**). The PLIF-HeatMap (Supplementary Material Table B) presents a similar picture.

3.4.2 Analysis of docking in the alternatives binding sites

When the interface site was selected in the TR (Supplementary Material Table A), all quinones finally were posed near the catalytic site, indicating a tendency to bind in this subsite (Supplementary Material Figure IV). However, when the same strategy was used for GR, it is noticeable that all quinones were placed in the middle of the interface site (Supplementary Material Figure IV). Earlier studies in GR

(Karplus & Schulz 1989) shown that a putative site with allosteric properties placed in the dimer interface should be considered as a putative binding site. Tridimensional and molecular dynamics analysis (Hikichi et al. 1995) shown that the GR dimer interface is quit adequate to lodge planar molecules as they are too the aryloxy-quinones here studied. However, if we take into account the scoring obtained for all of assayed sites, the dimer interface seems not to be the best for binding.

When the NADPH was used to center a putative binding site (Supplementary Material Table A), in the case of TR the scores of all quinones ranked in lower values than in the aryloxy-quinones site near the catalytic one described in the 3.4.1 Section. In principle, then, the NADPH site could be not considered as a secondary one for binding and for inhibition, remaining as more relevant the binding near the catalytic site. On the contrary, in the GR enzyme it seems to be a site with similar "appealing" for quinones than the active site, with similar scores for both sites. Any case, the NADPH site in GR seems to be a good alternative for binding. This result is in agreement with previous observations (Karplus, Pai & Schulz 1989). Then, for a molecule with a high binding energy either in the catalytic or the NADPH site in GR, it will be predictable a non-selective in TR inhibition.

3.4.3 3D Graphical analysis and modelling

3.4.3.1 Putative modeling of selective TR inhibitors

Taking the observations related to the catalytic and the NADPH sites together, it could be suggested that if a quinone must be designed as a non-competitive TR inhibitor, it must be bound near the catalytic site for TR but allowing the non-producing posing of TS_2. In addition, this compound must have low binding energies in the catalytic either the NADPH GR sites.

In the Figure 5, an hypothetical complex of a TR with **Nq-h** posed near the catalytic site (as described in the 3.4.1 Section) with the co-crystallized TS_2 in the crystallographic pose is shown. The TR-TS_2-**Nq-h** energy minimized model was used as putative virtual complex to show that there is enough room inside the catalytic site to lodge the TS_2 and the inhibitors. Furthermore, this model could agree with a non-competitive inhibition.

Based again in our results, to add selectivity against GR it will be necessary that the quinone, even if it will be posed in the NADPH site or in the catalytic site, the bound will be so weak to no interfere with

the GR activity. This is being sustained, for example in the case of **Nq-h**, by a low GR score, concomitantly with a very low GR inhibition capacity.

Moreover, if the aim of an anti-Chagasic drug should be to design optimal and selective TR inhibitors with maximal trypanocidal activity, structures like that of **Nq-h** could be used as leads to the improvement of the design.

3.4.3.2 Graphical analysis of best and selective TR inhibitors and comparison with the best trypanocidal assayed quinonic compounds.

In the Table 3, we add three more columns containing the score in TR and GR and finally, the ratio between both measurements (TR/GR) as a theoretical determination of the TR specificity (TRS).

If we take as good specificity a ratio over 1.1, the prediction of the TRS is that **Nq-h** and **Nq-g** are selective, and all other naphthoquinones are non-selective. We were successful into predict two of three TR selective inhibitors, and all (7) non-selective TR inhibitors. It was just only one failure into predict the **Nq-d** as non-selective (being selective). In view of this result we could be confident that the *in silico* methods have a very good capacity to predict if a molecule will be a selective TR inhibitor and to give an atomic description of the interaction.

Nq-g, **Nq-d** and **Nq-h** were furtherly analyzed and shown in the Figure 6 and 7 (TR and GR respectively). To do that, further energy minimization was done for the six complexes of those molecules docked in the TR and GR. The fact that - as it is clear in the Figure 6 - the place occupied by quinones in the docking is in the binding site of one of the carboxylate moieties of trypanothione, could have the meaning that the anchorage of the TS_2 in presence of the quinones is prevented, generating a bad and non-productive linkage.

The Figure 6d show clearly that the Lys62, Met400´and Ser464´are the most frequent and intense contacts for a TR specific binding. This conclusion reinforce the massive observations (PLIF analysis) made in the Section 3.4.1.

To compare with another interesting molecule with low score free energy to TR, we analyzed the **Nq-b**, the best trypanocidal molecule with low toxicity in the J-774 cells. In it best pose in TR, the nitro phenyl group is placed in the same region that the quinone ring in the **Nq-h** being the **Nq-b** quinone ring redirected towards the interface. The low score obtained for this **Nq-b** pose indicated that the nitro

group, with its charge localized in the nitrogen and oxygen atoms, is not adequate to bound this region in which the Lys62 and the Ser464´are sustaining the quinone rings of three best and specific TR ligand quinones above mentioned (**Nq-h**, **g** and **d**). The difference in the charge distribution (very concentrate in the nitro group and polarized in the oxygens of quinone rings) must be the key to understand the difference in their TR activity. Then, the same key moiety that gave to the quinones the best trypanocidal activity (a naphthoquinone with a nitrophenyl group), seems to be the responsible for a weak union to TR, making this design not corresponding to a selective TR inhibitor. In summary, we are showing that the action mechanism of naphthoquinones with a nitro group in it structure, making these molecules the best design for a non-toxic and trypanocidal compounds is not associated to the TR selective inhibition. Moreover, the lack of TR specificity could be explained too taking into account the global electrostatic charge of both TR and GR catalytic sites. The GR catalytic site has a global negative charge, and it will be -likely- very appealing to a negative charged nitro compound. However, the very good specific trypanocidal properties of the **Nq-b** compound is related to it good reactivity in the ROS mechanisms as well as some capacity to lower the toxicity with respect to nifurtimox.

To associate the previous consideration with the role of different residues in the TR selective inhibition, for the case of **Nq-h**, **Nq-g** and **Nq-d**, we could consider for one hand (Figure 6) the presence of a network of contacts with the quinonic ring sustained by the **Lys62, Ser464**' and **Leu399**' residues. The alpha naphthyl moieties (**Nq-h** and **Nq-g**) contribute to the posing and are oriented to the interface (**Nq-h**) or to the catalytic site (**Nq-g**). In the case of **Nq-d**, it phenyl moiety accomplish with the same role posing the quinonic ring near to the Lys62, Ser464'and Leu399'. On the other hand, the **Met400**, in the neighborhood of the bromine atoms (**Nq-h** and **Nq-g**) makes important surface contacts (Figure 6) giving better proper specificity to the TR anchorage. In the case of the non-brominated **Nq-d**, with its quinonic ring pointing to the polar region of Met400, a backbone donor H-bonding is giving the differential contact needed to confer TR specificity.

Once again, it was demonstrated for one hand that a molecule containing a naphthoquinone ring together to a brominated alfa naphthoxy or phenyloxy moiety seems to be a very good model to lead the design of a trypanocidal and non-toxic anti-trypanosomatid (e.g. anti-Chagas) drug. On the other hand, this pharmacological property was associated to a selective TR inhibition capacity mediated by a great number of contacts with the triad **Lys62**, **Ser464**' and **Met400,** with the **Leu399**´accomplishing an important and subtle role in the spatial orientation inside the site.

4. Conclusions

The aryloxy-quinones presented a tendency to have good docking scores in a new sub site inside the catalytic one, configuring a good model for the non-competitive type of inhibition obtained experimentally. In this putative binding of quinones, there is enough room for the substrate trypanothione that would be anchored but in a way which would interfere with the overall catalysis.

In the TR aryloxy-quinones binding site, the main contacts were detected with Lys62, Met400' and Ser464'. In GR, a similar sub site was occupied by quinones but there is a differential contact found in the Glu473' giving to this environment the electrostatic differential characteristic pointing to a selective binding in favor of TR.

For most of the compounds studied, a relationship between trypanocidal activity and TR inhibition could not be observed. However, three of the naphthoquinones, namely **Nq-h**, **Nq-g** and **Nq-d,** proved the hypothesis of a relationship between a good and non-toxic activity in *T. cruzi,* accompanied with low toxicity in mammalian cells associated with a specific TR inhibition.

Overall, our studies provided a more thorough understanding of the experimental trypanocidal results and revealed for selected compounds TR/GR as key enzymes in the action mechanisms of some aryloxy-quinones.

Interaction with other cellular targets cannot be discarded. Evidence for this is the very good and non-toxic activity of **Nq-b**, a nitro compound. A promising approach to optimize these compounds are *in silico* techniques such as for example the reverse docking that allows to find other targets that could contribute to the aryloxy-quinones trypanocidal action. A strategy involving the cycles of biochemical, parasitological and *in silico* assays, appears to be the best strategy for compound optimization and required to reach the final goal of a new anti-Chagas nontoxic drugs.

Acknowledgements

We are grateful to PEDECIBA-UDELAR Master in Bioinformatics ANII-Uruguay. KV thanks to PROMEP-México (Grant 103.5 -10-5345). CS thanks to financial support from FONDECYT (Research Grant) N° 1120128. Authors are very grateful to Professor Dr. R. Luise Krauth-Siegel (Biochemie-Zentrum der Universität Heidelberg (BZH)) for her valuable comments and technical and academic support in the TR assays.

References

Benites, J., Valderrama, J. A., Bettega, K., Pedrosa, R. C., Calderon, P. B. & Verrax, J. (2010). Biological evaluation of donor-acceptor aminonaphthoquinones as antitumor agents. *Eur J Med Chem, 45*, 6052-6057. doi: 10.1016/j.ejmech.2010.10.006

Berkholz, D. S., Faber, H. R., Savvides, S. N. & Karplus, P. A. (2008). Catalytic cycle of human glutathione reductase near 1 A resolution. *J Mol Biol , 382*, 371-384. doi: 10.1016/j.jmb.2008.06.083

Bern, C. (2011). Antitrypanosomal therapy for chronic Chagas' disease. *N Engl J Med, 364*, 2527-2534. doi: 10.1056/NEJMct1014204

Bern, C., Montgomery, S. P., Herwaldt, B. L., Rassi, A., Jr., Marin-Neto, J. A., Dantas, R. O., Maguire, J. H., Acquatella, H., Morillo, C., Kirchhoff, L. V., Gilman, R. H., Reyes, P. A., Salvatella, R. & Moore, A. C. (2007). Evaluation and treatment of chagas disease in the United States: a systematic review. *JAMA, 298*, 2171-2181. doi:10.1001/jama.298.18.2171

Bilzer M, R.L. Krauth-Siegel, R.H. Schirmer, T.P.M. Akerboom, H. Sies, G.E. Schulz (1984) Interaction of a glutathione S-conjugate with glutathione reductase *Eur J Biochem* ,138, 373–378. doi: 10.1111/j.1432-1033.1984.tb07925.x

Bond, C. S., Zhang, Y., Berriman, M., Cunningham, M. L., Fairlamb, A. H. & Hunter, W. N. (1999). Crystal structure of *Trypanosoma cruzi* trypanothione reductase in complex with trypanothione, and the structure-based discovery of new natural product inhibitors. *Structure*, 7, 81-89. doi: http://dx.doi.org/10.1016/S0969-2126(99)80011-2

Comini, M. A., Dirdjaja, N., Kaschel, M. & Krauth-Siegel, R. L. (2009). Preparative enzymatic synthesis of trypanothione and trypanothione analogues. *Int J Parasitol, 39*, 1059-1062. doi: 10.1016/j.ijpara.2009.05.002

Carraro, R., Iribarne, F., & Paulino, M. (2016). Analysis of cyclosporin A and a set of analogs as inhibitors of a T. cruzi cyclophilin by docking and molecular dynamics. *Journal of Biomolecular Structure & Dynamics*, *34*(2), 399–413. http://doi.org/10.1080/07391102.2015.1038584

de Molfetta, F. A., de Freitas, R. F., da Silva, A. B. & Montanari, C. A. (2009). Docking and molecular dynamics simulation of quinone compounds with trypanocidal activity. *J Mol Model, 15*, 1175-1184. doi: 10.1007/s00894-009-0468-3

de Paula da Silva, C. H. T., Bernardes, L. S. C., da Silva, V. B., Zani, C. L., & Carvalho, I. (2012). Novel aryl β-aminocarbonyl derivatives as inhibitors of Trypanosoma cruzi trypanothione reductase: binding mode revised by docking and GRIND2-based 3D-QSAR procedures. *Journal of Biomolecular Structure & Dynamics*, *29*(6), 702–16. http://doi.org/10.1080/07391102.2011.672633

el-Waer, A., Douglas, K. T., Smith, K. & Fairlamb, A. H. (1991). Synthesis of *N*-benzyloxycarbonyl-L-cysteinylglycine 3-dimethylaminopropylamide disulfide: a cheap and convenient new assay for trypanothione reductase. *Anal Biochem, 198*, 212-216. doi:10.1016/0003-2697(91)90531-W

Fairlamb, A. H., Blackburn, P., Ulrich, P., Chait, B. T. & Cerami, A. (1985). Trypanothione: a novel bis(glutathionyl)spermidine cofactor for glutathione reductase in trypanosomatids. *Science, 227*, 1485-1487. doi: 10.1126/science.3883489

Fernandez-Blanco, C., Font, G. & Ruiz, M. J. (2016). Interaction effects of enniatin B, deoxinivalenol and alternariol in Caco-2 cells. *Toxicol Lett, 241*, 38-48. doi: 10.1016/j.toxlet.2015.11.005

Gonzalez-Chavez, Z., Olin-Sandoval, V., Rodriguez-Zavala, J. S., Moreno-Sanchez, R. & Saavedra, E. (2015). Metabolic control analysis of the *Trypanosoma cruzi* peroxide detoxification pathway identifies tryparedoxin as a suitable drug target. *Biochim Biophys Acta, 1850*, 263-273. doi:10.1016/j.bbagen.2014.10.029

Gutteridge, J. M. & Halliwell, B. (2000). Free radicals and antioxidants in the year 2000. A historical look to the future. *Ann N Y Acad Sci, 899*, 136-147. doi: 10.1111/j.1749-6632.2000.tb06182.x

Halgren, T. A. (1996). Merck molecular force field .1. Basis, form, scope, parameterization, and performance of MMFF94. *J Comput Chem, 17*, 490-519. doi: 10.1002/(SICI)1096-987X(199604)17:5/6<490::AID-JCC1>3.0.CO;2-P

Halgren, T. A. (1996). Merck molecular force field .5. Extension of MMFF94 using experimental data, additional computational data, and empirical rules. *J Comput Chem, 17*, 616-641. doi: 10.1002/(SICI)1096-987X(199604)17:5/6<616::AID-JCC5>3.0.CO;2-X

Henry, T. R. & Wallace, K. B. (1996). Differential mechanisms of cell killing by redox cycling and arylating quinones. *Arch Toxicol, 70*, 482-489. doi: 10.1007/s002040050302

Hikichi, N., Paulino, M., Hansz, M. & Tapia, O. (1995). A Molecular-Dynamics Study of Glutathione-Reductase. *J Mol Struct-Theochem, 335*, 243-254. doi: 10.1016/0166-1280(94)04005-D

Hoelz, L. V. B., Leal, V. F., Rodrigues, C. R., Pascutti, P. G., Albuquerque, M. G., Muri, E. M. F., & Dias, L. R. S. (2015). Molecular dynamics simulations of the free and inhibitor-bound cruzain systems in aqueous solvent: insights on the inhibition mechanism in acidic pH. *Journal of Biomolecular Structure & Dynamics*, 1–10. http://doi.org/10.1080/07391102.2015.1100139

Iribarne, F., Paulino, M., Aguilera, S. & Tapia, O. (2009). Assaying phenothiazine derivatives as trypanothione reductase and glutathione reductase inhibitors by theoretical docking and molecular dynamics studies. *J Mol Graph Model, 28*, 371-381. doi: 10.1016/j.jmgm.2009.09.003

Janes, W. & Schulz, G. E. (1990). The binding of the retro-analogue of glutathione disulfide to glutathione reductase. *J Biol Chem, 265*, 10443-10445. doi: 10.2210/pdb4gr1/pdb

Karplus, P. A., Pai, E. F. & Schulz, G. E. (1989). A crystallographic study of the glutathione binding site of glutathione reductase at 0.3-nm resolution. *Eur J Biochem, 178*, 693-703. doi: 10.1111/j.1432-1033.1989.tb14500.x

Karplus, P. A. & Schulz, G. E. (1987). Refined structure of glutathione reductase at 1.54 Å resolution. *J Mol Biol, 195*, 701-729. doi: 10.2210/pdb3grs/pdb

Karplus, P. A. & Schulz, G. E. (1989). Substrate binding and catalysis by glutathione reductase as derived from refined enzyme: substrate crystal structures at 2 Å resolution. *J Mol Biol, 210*, 163-180. doi:10.1016/0022-2836(89)90298-2

Kovacic, P. (2007). Unifying mechanism for anticancer agents involving electron transfer and oxidative stress: clinical implications. *Med Hypotheses, 69*, 510-516. doi: 10.1016/j.mehy.2006.08.046

Labute, P. (2010). LowModeMD--implicit low-mode velocity filtering applied to conformational search of macrocycles and protein loops. *J Chem Inf Model, 50*, 792-800. doi: 10.1021/ci900508k.

Manoel-Caetano Fda, S. & Silva, A. E. (2007). Implications of genetic variability of *Trypanosoma cruzi* for the pathogenesis of Chagas disease. *Cad Saude Publica, 23*, 2263-2274. doi: 10.1590/S0102-311X2007001000002

Maran, E., Fernandez, M., Barbieri, P., Font, G. & Ruiz, M. J. (2009). Effects of four carbamate compounds on antioxidant parameters. *Ecotoxicol Environ Saf, 72*, 922-930. doi: 10.1016/j.ecoenv.2008.01.018

Molina, I., Gomez i Prat, J., Salvador, F., Trevino, B., Sulleiro, E., Serre, N., Pou, D., Roure, S., Cabezos, J., Valerio, L., Blanco-Grau, A., Sanchez-Montalva, A., Vidal, X. & Pahissa, A. (2014). Randomized trial of posaconazole and benznidazole for chronic Chagas' disease. *N Engl J Med, 370*, 1899-1908. doi: 10.1056/NEJMoa1313122

Nordhoff, A., Bucheler, U. S., Werner, D. & Schirmer, R. H. (1993). Folding of the four domains and dimerization are impaired by the Gly446-->Glu exchange in human glutathione reductase. Implications for the design of antiparasitic drugs. *Biochemistry, 32*, 4060-4066. doi: 10.1021/bi00066a029

O'Brien, P. J. (1991). Molecular mechanisms of quinone cytotoxicity. *Chem Biol Interac, 80*, 1-41. doi: 10.1016/0009-2797(91)90029-7

Pai, E. F., Karplus, P. A. & Schulz, G. E. (1988). Crystallographic analysis of the binding of NADPH, NADPH fragments, and NADPH analogues to glutathione reductase. *Biochemistry, 27*, 4465-4474. doi: 10.1021/bi00412a038

Pai, E. F. & Schulz, G. E. (1983). The catalytic mechanism of glutathione reductase as derived from x-ray diffraction analyses of reaction intermediates. *J Biol Chem, 258*, 1752-1757. Retrieved from http://www.jbc.org/content/258/3/1752.abstract#cited-by

Paulino, M., Alvareda, E. M., Denis, P. A., Barreiro, E. J., Sperandio da Silva, G. M., Dubin, M., Gastellu, C., Aguilera, S. & Tapia, O. (2008). Studies of trypanocidal (inhibitory) power of naphthoquinones: evaluation of quantum chemical molecular descriptors for structure-activity relationships. *Eur J Med Chem, 43*, 2238-2246. doi: 10.1016/j.ejmech.2007.12.023

Paulino, M., Iribarne, F., Dubin, M., Aguilera-Morales, S., Tapia, O. & Stoppani, A. O. (2005). The chemotherapy of chagas' disease: an overview. *Mini Rev Med Chem, 5*, 499-519. doi: 10.2174/1389557053765565

Persch, E., Bryson, S., Todoroff, N. K., Eberle, C., Thelemann, J., Dirdjaja, N., Kaiser, M., Weber, M., Derbani, H., Brun, R., Schneider, G., Pai, E. F., Krauth-Siegel, R. L. & Diederich, F. (2014). Binding to large enzyme pockets: small-molecule inhibitors of trypanothione reductase. *Chem Med Chem, 9*, 1880-1891. doi: 10.1002/cmdc.201402032

Prati, F., Bergamini, C., Molina, M. T., Falchi, F., Cavalli, A., Kaiser, M., Brun, R., Fato, R. & Bolognesi, M. L. (2015). 2-Phenoxy-1,4-naphthoquinones: From a Multitarget Antitrypanosomal to a Potential Antitumor Profile. *J Med Chem, 58*, 6422-6434. doi: 10.1021/acs.jmedchem.5b00748

Rassi, A., Jr., Rassi, A. & Marin-Neto, J. A. (2010). Chagas disease. *Lancet, 375*, 1388-1402. doi: 10.1016/S0140-6736(10)60061-X

Salas, C. O., Faundez, M., Morello, A., Maya, J. D. & Tapia, R. A. (2011). Natural and synthetic naphthoquinones active against *Trypanosoma cruzi*: an initial step towards new drugs for Chagas disease. *Curr Med Chem, 18*, 144-161. doi: 10.2174/092986711793979779

Salmon-Chemin, L., Buisine, E., Yardley, V., Kohler, S., Debreu, M. A., Landry, V., Sergheraert, C., Croft, S. L., Krauth-Siegel, R. L. & Davioud-Charvet, E. (2001). 2- and 3-substituted 1,4-naphthoquinone derivatives as subversive substrates of trypanothione reductase and lipoamide dehydrogenase from *Trypanosoma cruzi*: synthesis and correlation between redox cycling activities and in vitro cytotoxicity. *J Med Chem, 44*, 548-565. doi: 10.1021/jm001079l

Savvides SN, Karplus PA (1996) Kinetics and crystallographic analysis of human glutathione reductase in complex with a xanthene inhibitor. *J Biol Chem*, 271(14), 8101-8107. doi: 10.1074/jbc.271.14.8101

Turrens, J. F. (2004). Oxidative stress and antioxidant defenses: a target for the treatment of diseases caused by parasitic protozoa. *Mol Aspects Med, 25*, 211-220. doi: 10.1016/j.mam.2004.02.021

Udatha, D. B., Sugaya, N., Olsson, L. & Panagiotou, G. (2012). How well do the substrates KISS the enzyme? Molecular docking program selection for feruloyl esterases. *Sci Rep, 2*, 323. doi: 10.1038/srep00323

Vazquez, K., Espinosa-Bustos, C., Soto-Delgado, J., Tapia, R. A., Varela, J., Birriel, E., Segura, R., Pizarro, J., Cerecetto, H., Gonzalez, M., Paulino, M. & Salas, C. O. (2015). New aryloxy-quinone derivatives as potential antiChagasic agents: synthesis, trypanocidal activity, electrochemical properties, pharmacophore elucidation and 3D-QSAR analysis. *RSC Advances, 5*, 65153-65166. doi: 10.1039/C5RA10122K

Viotti, R., Vigliano, C., Lococo, B., Bertocchi, G., Petti, M., Alvarez, M. G., Postan, M. & Armenti, A. (2006). Long-term cardiac outcomes of treating chronic Chagas disease with benznidazole versus no treatment: a nonrandomized trial. *Ann Intern Med, 144*, 724-734. doi:10.7326/0003-4819-144-10-200605160-00006

Walsh, C., Bradley, M. & Nadeau, K. (1991). Molecular studies on trypanothione reductase, a target for antiparasitic drugs. *Trends Biochem Sci, 16*, 305-309. doi: 10.1016/0968-0004(91)90124-E

WHO (2011). Working to overcome the global impact of neglected tropical diseases - Summary. *Releve epidemiologique hebdomadaire / Section d'hygiene du Secretariat de la Societe des Nations = Weekly epidemiological record / Health Section of the Secretariat of the League of Nations, 86*, 113-120. doi: 10.1016/S0140-6736(09)61877

Woodcock, J. & Woosley, R. (2008). The FDA critical path initiative and its influence on new drug development. *Annu Rev Med, 59*, 1-12. doi: 10.1146/annurev.med.59.090506.155819

Worthington, D. J. & Rosemeyer, M. A. (1974). Glutathione Reductase from Human Erythrocytes. E*ur. J Biochem,* 48, 167- 177. doi: 10.1111/j.1432-1033.1974.tb03754.x

Yun, O., Lima, M. A., Ellman, T., Chambi, W., Castillo, S., Flevaud, L., Roddy, P., Parreno, F., Albajar Vinas, P. & Palma, P. P. (2009). Feasibility, drug safety, and effectiveness of etiological treatment programs for Chagas disease in Honduras, Guatemala, and Bolivia: 10-year experience of Medicines Sans Frontiers. *PLoS Negl Trop Dis, 3*, e488. doi: 10.1371/journal.pntd.0000488

Zani, C. L. & Fairlamb, A. H. (2003). 8-Methoxy-naphtho[2,3-b]thiophen-4,9-quinone, a non-competitive inhibitor of trypanothione reductase. *Mem Inst Oswaldo Cruz 98*: 565-568. Retrieved from http://dx.doi.org/10.1590/S0074-02762003000400026

CAPTIONS FOR THE FIGURES

Figure 1. Chemical structures of aryloxy-quinones with trypanocidal interesting activities.

Figure 2. Catalytic site (purple) and interface site (green) of A) trypanothione reductase and B) glutathione reductase. In the top left corner of each figure are shown the electrostatic surfaces of the TR (SC-TR) and GR (SC-GR) catalytic sites. Electrostatic positive and negative surfaces were colored in red and blue respectively.

In the bottom left corner of Figures 2A and 2B the docked naphthoquinones in the catalytic site of trypanothione reductase and glutathione reductase were shown. In red: molecule conformers with high scores ranging from -13.4 to -10.1 kcal/mol. In yellow: molecule conformers with low scores ranging lower scored from -10.1 to -5.3 kcal/mol.

Figure 3. Barcode display analysis of PLIF results. The horizontal rods correspond to each of the studied compounds. A black rod indicates the presence of an interaction with residues shown in the X-axis at the bottom of each graph. **3a.** Barcode display in TR. **3b.** Barcode display in GR.

Figure 4. Histogram (Population Display) of PLIF results showing the number of ligands (Y-axis) with which each residue (plotted in the X-axis) interacts. **4a.** Population display in TR. **4b.** Population display in GR.

Figure 5. Putative complex TR-TS_2-**Nq-h** . **Top**: Trypanothione reductase draw of backbone in orange and magenta ribbons. A dotted light pink surface is showing the catalytic site and interface sourroundings. A black rectangle is amplified in the middle: the TS_2 is shown in blue rods. The **Nq-h** quinone is shown in green rods. **Right:** 2D picture of the Ligand Interactions analysis showing the contacts made by **Nq-h** in TR. Green arrows indicate H-bond side chain interactions. Blue light shadows are places where there is ligand exposition.

Figure 6. The best scored poses in trypanothione reductase of a) **Nq-h** (cyan rods), b) **Nq-g** (magenta rods) and c) **Nq-d** (green rods) d) Ligand interaction fingerprint report: Lys62: ChDon and Surf; Thr66: ChDon; Asn433': ChDon and Surf; Leu399': BkDon; Met400': BkDon and Surf; His401': ChDon; Lys402': ChDon; Asp432': Surf; His461' :ChDon; Thr463': BkDon; Ser464': BkDon and

ChDon. ChDon = side-chain atoms act as H-bond acceptors or donors. BkDon = backbone atoms act as H-bond acceptors or donors. Surf = surface contact interactions

Figure 7. The best scored poses in glutathione reductase of a) **Nq-h** (cyan rods), b) **Nq-g** (magenta rods) and c) **Nq-d** (green rods). Ligand interaction fingerprint report: Lys67(Lys62 in TR): ChDon; Asn71(Thr66 in TR): ChDon, Tyr106: ChDon ; Tyr114: Surf; Ile343: Surf; Arg347: Surf; Met406'(Leu399´in TR): BkDon; Leu438'(Asp432´in TR): Surf; His467'(His461´in TR): ChDon and Surf; Thr469'(Thr463´in TR): BkDon; Ser470'(Ser464´in TR): BkDon; Glu473': Surf. Note that these quinones have no interaction with Ile113,Thr404',Thr476'. ChDon = side-chain atoms act as H-bond acceptor or donors. BkDon =backbone atoms act as H-bond acceptors or donors. Surf = surface contact interactions

2-aryloxy-naphthoquinones

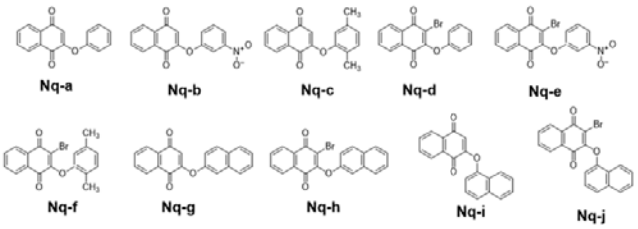

7-aryloxy-quinolinquinones

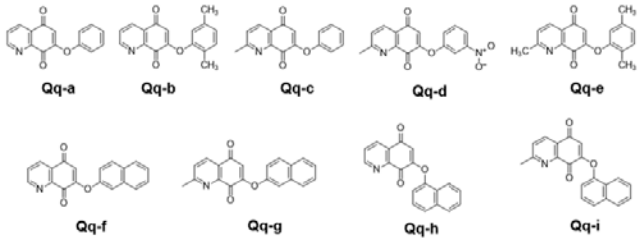

6-aryloxy-furonaphthoquinones

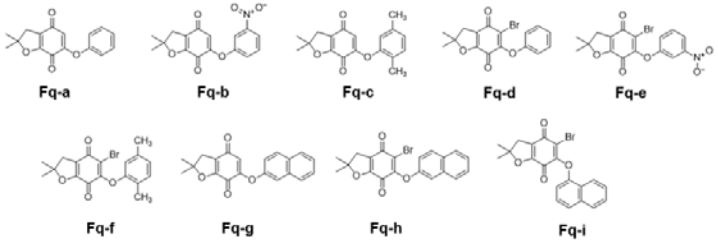

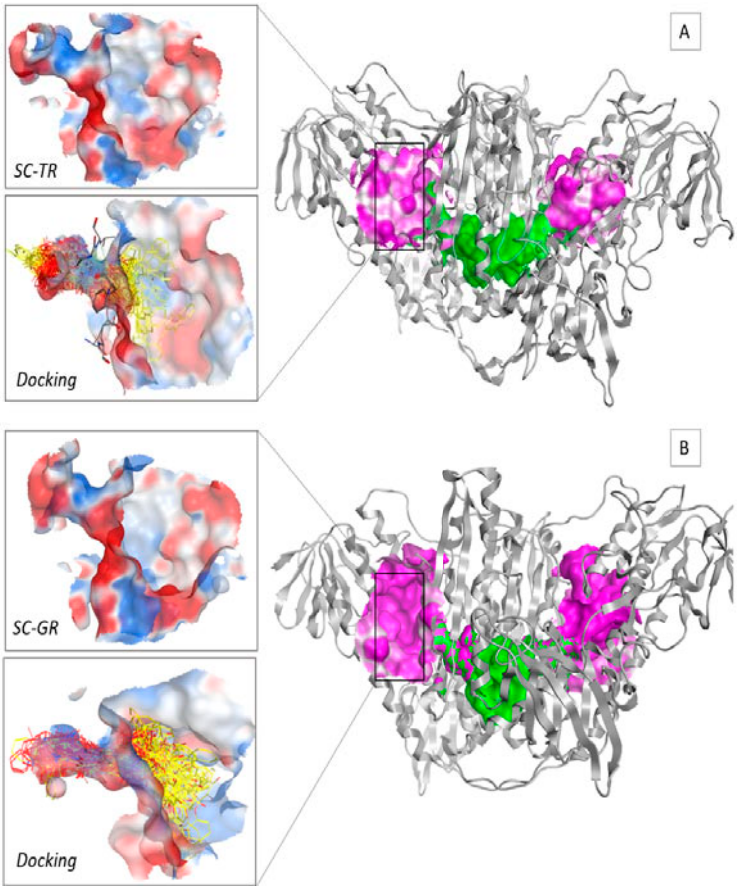

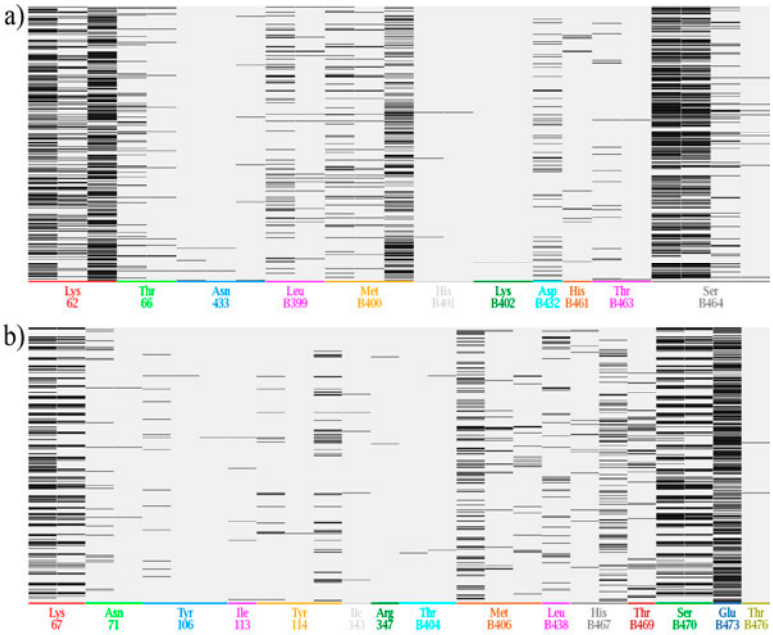

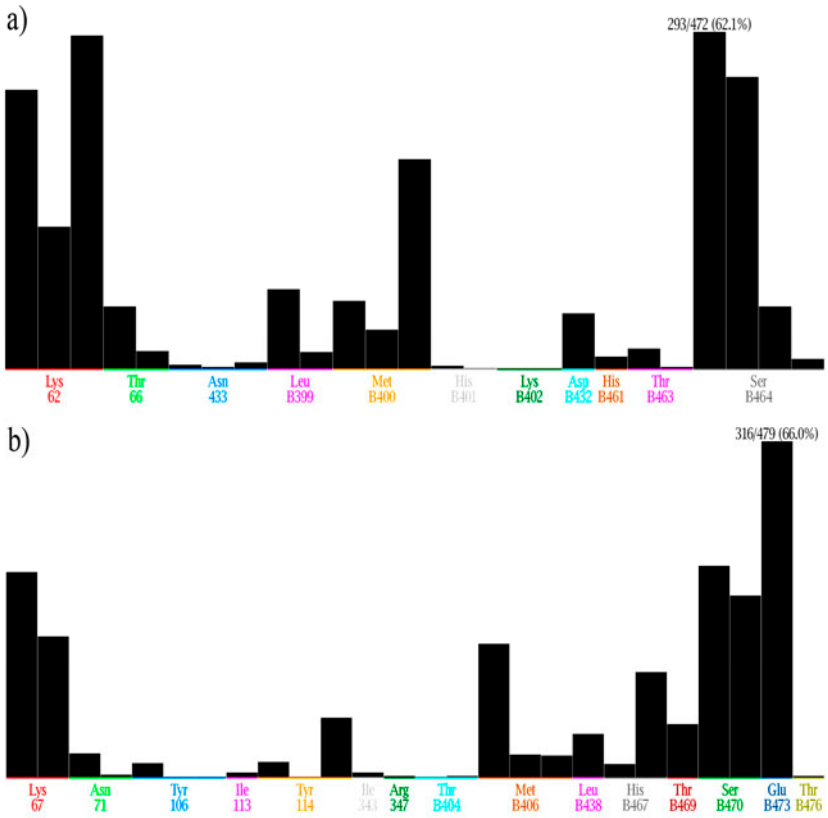

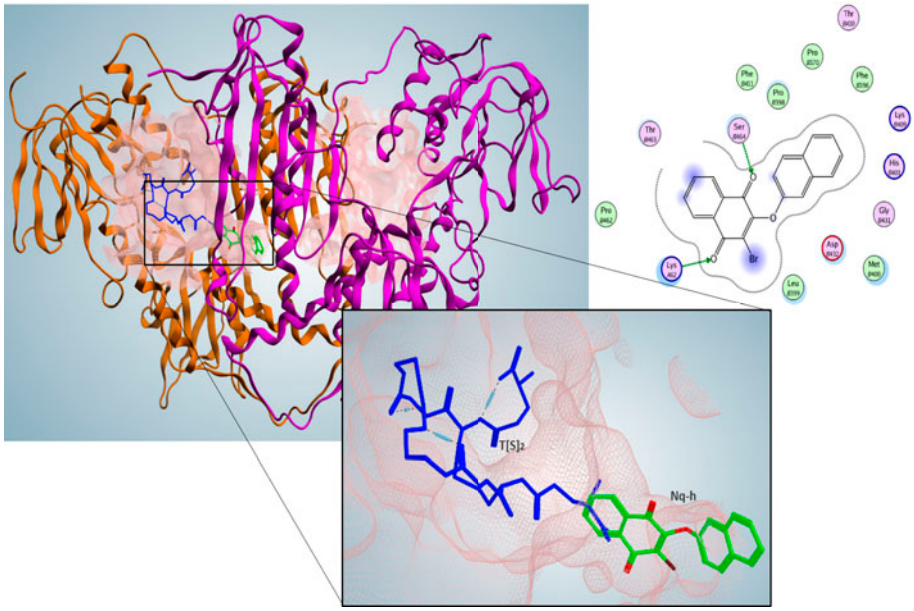

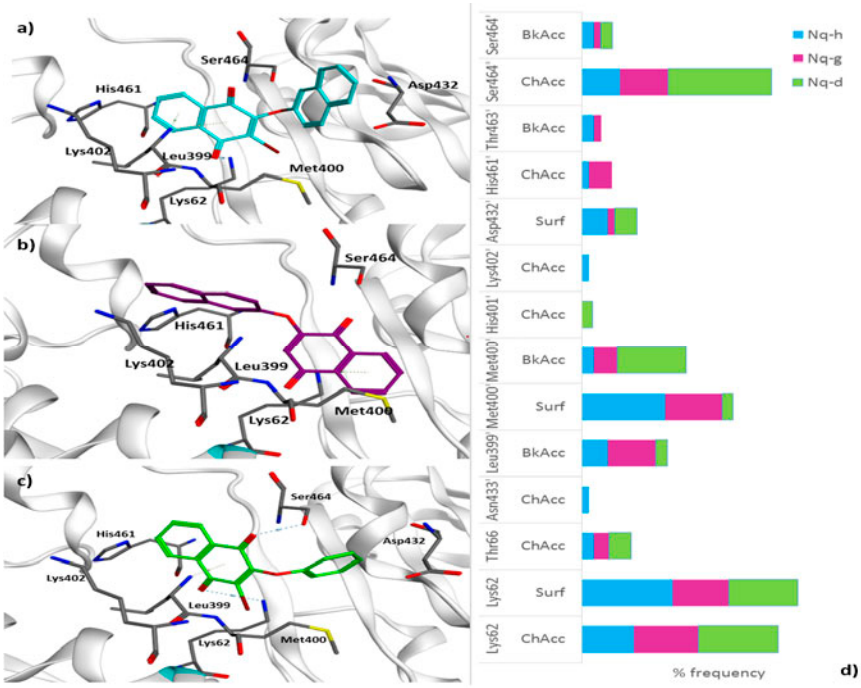

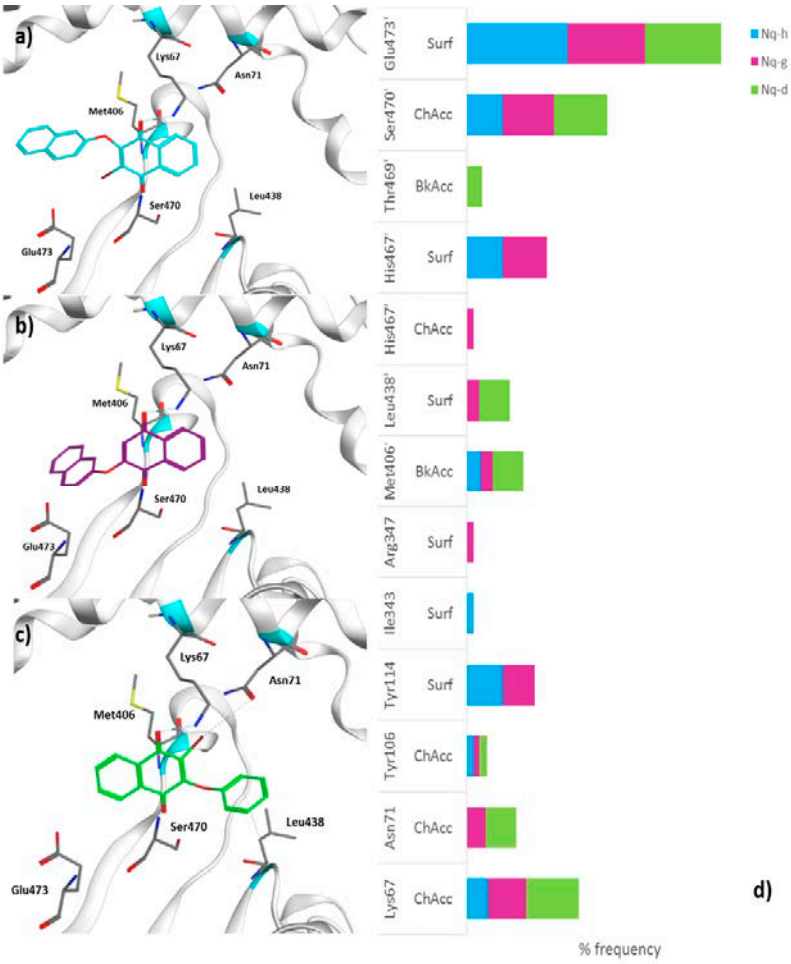

Table 1: First column, coded name of quinones. Second and Third columns: IC_{50} for the *T. cruzi* growth inhibition and cytotoxicity in J-774 IC_{50} in µM. Fourth and Fifth columns: percentages of trypanothione and glutathione reductase inhibition and in parentheses are annotated the related concentrations in µM. * Data are from Vazquez et al 2015.

Molecule	IC_{50} ***T cruzi*** Epimastigote*	J-774 IC_{50}*	% TR inhibition	% GR inhibition
Naphthoquinones				
Nq-a	0.05 ± 0.04	< 12.5	62 % (5)	50 % (7.32)
Nq-b	0.02 ± 0.01	12.5	57 % (100)	50 % (1.4)
Nq-c	0.17 ± 0.05	< 12.5	46 % (2.5)	50 % (3.9)
Nq-d	0.11 ± 0.04	18	53 % (5)	50 % (>100)
Nq-e	0.11 ± 0.04	46	41 % (10)	50 % (>100)
Nq-f	insoluble	insoluble	insoluble	50 % (>100)
Nq-g	0.15 ± 0.04	< 12.5	43 % (2.5)	50 % (>100)
Nq-h	0.14 ± 0.05	< 12.5	64 % (5)	50 % (>100)
Nq-i	0.17 ± 0.04	< 12.5	precipitated	50 % (>100)
Nq-j	0.17 ± 0.06	19	precipitated	50 % (>100)
Furanquinones				
Fq-a	1.00 ± 0.02	21	24 % (12.5)	50 % (>100)
Fq-b	2.30 ± 0.03	61	4 % (1.5)	50 % (>100)
Fq-c	0.54 ± 0.13	44	25 % (10)	50 % (>100)
Quinolinquinones				
Qq-b	2.30 ± 0.03	18	52 % (50)	50 % (>100)
Qq-c	0.14 ± 0.05	12.5	65 % (10)	50 % (>100)
Qq-d	0.44 ± 0.09	12.5	46 % (10)	50 % (1.69)

Qq-e	0.23 ± 0.07	< 12.5	31 % (3.1)	50 % (3.33)
Qq-g	0.98 ± 0.17	16	35 % (12.5)	50 % (6.32)
Qq-i	0.17 ± 0.05	< 12.5	36 % (10)	50 % (3.09)
Nifurtimox	7.00 ± 0.3	316 ± 0.5	-	-

Table 2. Aryloxy-naphthoquinone derivatives kinetics of TR inhibition		
Molecule	Ki (µM)	Inhibition kinetics
Nq-h	1,1	Non competitive
Qq-b	6,0	Non competitive
Fq-c	18,5	Non competitive

Table 3 Summary of the structural characteristics for the assayed sets of naphtoquinones (**Columns 2 to 6**). **Columns 7 and 8**: color coded *T. cruzi* inhibition growth and J-774 measurements (Vazquez et al. 2015): *T. cruzi* growth inhibition was considered TRYPANOCIDAL (GREEN) for compound concentrations below 0.17µM; MEDIUM for concentrations between 0.17 and 7 µM and LOW (RED) those equal or higher than 7 µM (that of Nfx). **Columns 9 and 10**: color coded TR and GR inhibition results. TR inhibition was considered good (GREEN) when inhibitions of more than 43% were detected with concentrations below 5µM. All other cases were considered low (RED); GR inhibition was considered low (RED) when a 50% inhibition was obtained for concentrations above 100µM; all other cases were considered a low inhibition (GREEN). **Column 11**: Index of selectivity (IS) evaluated from data of Table 1 for the *T. cruzi* inhibition as the ratio between the J-774 by the *T. cruzi* growth inhibition concentrations. Values over 90 were considered as SELECTIVES (GREEN), between 45 and 90 MEDIUM SELECTIVITY (YELLOW) and BAD SELECTIVITY (RED) (<45). **Column 12**: The Index of Selectivity for the inhibition of TR (TRS) was calculated as the ratio between the values in the fourth by the fifth columns of the Table 1 and were classified as SELECTIVE TR INIHIBITION (GREEN) when a value over 20 was obtained. **Column 13:** the ratio of free energies in TR by GR (data from Supplementary Material Table A). Selectivity is assigned to rates over 1.11 (GREEN). **Last two columns:** main questions are YES/NO answered.

Molecule	Nitro	Br	naphtyloxy	phenyloxy	methylphenyloxy	*T.cruzi* activity	Putative human	TR inhibition	GR inhibition	*T. cruzi* selectivity (IS)	TR selectivity (TRS)	In Silico free energies	Inhibt *T. cruzi* with low toxicity?	Inhibit selectively TR?
Nq-a				x		highly tripapnocidal	non toxic	inhibition	inhibition	250	1.5	1	YES	NO
Nq-b	x			x		higher tripanocidal activity	non toxic	low inhibition	inhibition	1250	0.01	1.05	YES	NO
Nq-c					x	tripanocidal	medium toxicity	inhibition	inhibition	74	1.4	1.01	YES	NO
Nq-d		x		x		tripanocidal	non toxic	inhibition	low inhibition	164	20	0.93	YES	YES
Nq-e	x	x		x		tripanocidal	non toxic	low inhibition	low inhibition	418	10	0.99	YES	NO
Nq-f		x			x	ins	ins	ins	low inhibition	—	—	1.01		
Nq-g			x α			tripanocidal	medium toxicity	inhibition	low inhibition	83	40	1.11	YES	YES
Nq-h		x	x α			tripanocidal	medium toxicity	inhibition	low inhibition	89	20	1.2	YES	YES
Nq-i			x β			tripanocidal	medium toxicity	ins	low inhibition	74	—	1.03	YES	NO
Nq-j		x	x β			tripanocidal	non toxic	ins	low inhibition	112	—	0.89	YES	NO

Table 4: All combinations of docking conditions assayed to docking validation. Binding energy values are in kcal/mol

Placement	Alfa PMI		TM	
Score Function	Affinity dG	London dG	Affinity dG	London dG
Naphthoquinones	-6.72 to -5.6	-13.6 to -0.69	-6.96 to -1.74	-7 to -1.65
Furanequinones	-7.11 to -5.5	-13.7 to -2.99	-7 to -1.65	-10.83 to -6
Quinolinequinones	-6.88 to -5.69	-13.7 to -2.29	-6.65 to -1.7	-10 to -5.85

TABLE 5. PLIF-ContactMap: Contact percentage detected by PLIF between a given aminoacid and all conformers of each quinone in TR and GR. **X-Axis:** TR (grey) and GR (yellow) contact codes are detailed: Side chain H-acceptor (ChAcc), Backbone H-acceptor (BkAcc), and Surface contact (Surf). Blocks are colored by means of a color gradient from blue (low percentage of contact) to red (high percentage of contact). Red blocks indicate a highly frequent contacts. Black frames were used to groupe similar residues in TR/GR. **Y-axis:** aryloxy-quinones set.

TR	GR	Lys62			Lys67		Thr66		Asn71		Tyr106			Ile113	Tyr114			Ile343	Arg347	Asn433			Leu399'		Met406'			Met400'			His401'		Thr404'		Lys402'		Asp432'	Leu348'	His461'		His467'		Thr463'		Thr469'	Ser464'					Ser470'		Glu473'	Thr476'
Molecule		ChAcc1	ChAcc2	Surf	ChAcc1	ChAcc2	ChAcc1	ChAcc2	ChAcc1	ChAcc2	ChAcc1	ChAcc2	Surf	Surf	ChAcc1	ChAcc2	Surf	Surf	Surf	ChAcc1	ChAcc2	Surf	BkAcc1	BkAcc2	ChAcc1	ChAcc2	Surf	BkAcc1	BkAcc2	ChAcc1	ChAcc2	Surf	ChAcc1	ChAcc2	Surf	BkAcc	Surf	ChAcc1	ChAcc2	Surf	ChAcc1	ChAcc2	Surf	BkAcc	ChAcc1	ChAcc2	BkAcc	BkAcc	ChAcc1	ChAcc2	Surf	ChAcc1
Nq-a		50	28	44	27	27	22	22	13	0	0	0	0	0	0	0	0	0	0	0	0	6	17	0	33	7	0	17	6	28	0	0	0	0	0	0	7	0	7	0	0	0	0	61	61	11	0	40	33	60	0
Nq-b		48	22	52	36	21	9	4	14	0	0	0	0	0	0	0	0	0	0	0	0	0	17	9	21	0	0	13	9	22	0	0	0	0	0	0	9	7	9	0	14	0	0	0	65	61	13	0	36	36	57	0
Nq-c		52	26	83	38	33	4	0	0	0	5	5	0	0	5	0	10	0	0	0	0	4	13	4	19	0	10	9	4	39	0	0	0	5	0	0	13	0	0	0	19	13	0	5	65	52	9	0	43	38	57	0
Nq-d		54	15	46	44	19	15	8	25	0	6	0	0	0	0	0	0	0	0	0	0	0	8	0	25	0	0	8	8	46	8	0	0	0	0	0	15	25	0	0	0	0	0	13	69	62	8	0	44	38	63	0
Nq-e		64	14	64	40	33	21	7	7	0	0	0	0	0	0	0	0	0	0	7	7	0	7	0	27	0	0	7	7	43	0	0	0	0	0	0	14	13	0	0	13	0	0	20	71	71	21	0	47	40	67	0
Nq-f		50	6	88	33	28	6	0	0	0	0	0	0	6	6	0	11	0	0	6	0	6	6	0	28	0	6	13	0	56	0	0	0	0	0	0	19	0	0	0	17	13	6	17	75	69	13	6	33	33	61	0
Nq-g		44	28	39	32	21	11	6	16	0	5	0	0	0	0	0	26	0	5	0	0	0	33	6	11	0	0	17	11	39	0	0	0	0	0	0	6	11	17	5	37	6	0	0	33	28	6	0	42	42	63	0
Nq-h		36	27	64	18	18	9	9	0	0	6	0	0	0	0	0	29	6	0	5	0	0	18	5	12	0	0	9	5	55	0	0	0	0	5	5	18	0	5	0	29	9	0	0	27	18	9	0	29	29	82	0
Nq-i		50	15	75	53	41	0	0	6	0	0	0	0	0	0	0	0	0	0	0	0	0	10	0	35	0	0	5	5	45	0	0	0	0	0	0	10	47	0	6	6	5	0	0	65	50	15	0	65	53	65	0
Nq-j		38	25	81	33	22	13	6	0	0	6	0	0	0	0	0	11	0	0	6	6	0	0	0	33	17	0	0	0	81	0	0	0	0	0	0	13	6	0	6	17	6	0	22	69	50	19	0	28	28	67	0
Qq-a		54	23	38	43	29	23	8	7	0	0	0	0	0	0	0	0	0	0	0	0	0	8	0	43	14	0	15	8	23	0	0	0	0	0	0	8	0	0	7	7	8	0	7	85	77	8	0	50	36	57	0
Qq-b		56	33	56	50	45	11	0	0	0	5	0	0	0	5	0	5	0	0	0	0	0	28	11	10	0	5	22	17	17	22	0	0	0	0	0	5	0	0	20	0	6	10	0	61	50	6	55	45	50	0
Qq-c		60	60	40	45	27	10	0	9	0	0	0	0	0	0	0	0	0	0	0	0	0	20	10	18	9	9	10	10	10	0	0	0	0	0	0	0	0	10	9	27	0	0	0	70	70	0	0	36	36	45	0
Qq-d		50	38	63	38	15	0	0	8	0	0	0	0	8	0	0	8	0	0	0	0	0	19	13	31	0	8	13	6	13	0	0	0	0	0	0	8	13	0	38	6	0	0	56	50	13	0	23	23	46	0
Qq-e		55	30	55	38	29	10	0	0	0	0	0	0	0	0	0	14	0	0	0	0	0	15	0	19	5	14	10	10	20	0	0	5	5	0	0	0	5	0	0	33	0	0	0	50	45	5	0	38	38	62	0
Qq-f		35	24	65	39	22	24	6	11	0	6	0	0	0	17	0	17	6	0	0	0	0	18	6	17	0	0	29	12	59	0	0	0	0	0	0	24	11	0	0	22	6	0	0	35	24	18	6	44	39	50	6
Qq-g		33	28	44	28	22	6	0	6	0	6	0	0	0	17	6	22	0	0	0	0	0	28	6	22	0	0	6	6	44	0	0	0	0	0	0	6	6	11	0	22	11	0	0	33	33	0	0	33	28	72	0
Qq-h		41	18	71	53	47	0	0	0	0	0	0	0	0	0	0	0	0	0	0	0	6	12	0	33	0	0	6	6	41	6	0	0	0	0	0	24	33	0	0	13	0	0	7	53	47	6	0	67	47	53	0
Qq-i		72	44	67	47	42	6	6	5	5	0	0	0	5	5	0	16	0	0	0	0	6	17	0	21	0	0	17	17	44	0	0	0	0	0	0	17	11	0	5	21	0	0	5	50	39	11	0	68	63	63	0
Fq-a		69	31	46	43	21	0	0	0	0	0	0	0	0	0	0	0	0	0	0	0	0	23	0	50	7	7	23	15	8	0	0	0	0	0	0	8	0	0	0	7	0	0	14	77	62	8	0	43	29	71	0
Fq-b		76	18	59	43	43	0	0	0	0	7	0	0	0	0	0	0	0	0	0	0	0	12	0	21	0	0	18	12	18	0	0	0	0	0	0	18	0	0	0	14	0	0	0	71	59	6	0	50	43	71	0
Fq-c		76	35	82	50	44	18	0	0	0	0	0	0	0	6	0	6	6	0	0	0	0	18	0	31	6	0	6	6	29	0	0	0	0	0	0	6	0	0	0	38	0	0	13	71	65	12	0	50	50	69	0
Fq-d		50	33	58	50	36	33	8	0	0	7	0	0	0	0	0	7	0	0	0	0	0	0	0	29	7	0	8	0	50	0	0	0	0	0	0	8	14	0	7	14	0	0	29	100	83	17	8	50	36	86	0
Fq-e		53	29	71	38	19	18	6	5	5	5	0	0	0	0	0	19	0	0	0	0	0	0	0	33	10	5	12	0	53	0	0	0	0	0	0	12	5	0	10	24	0	0	24	88	82	24	12	33	29	76	0
Fq-f		50	8	67	65	25	17	0	0	0	0	0	0	5	0	0	0	0	0	0	0	0	0	0	35	10	30	8	0	50	0	0	0	0	0	0	8	0	0	0	15	8	0	30	83	83	25	8	35	25	70	0
Fq-g		53	29	65	37	16	18	6	5	5	5	0	0	0	5	0	32	5	0	0	0	0	41	0	26	0	0	29	18	29	0	0	0	0	0	0	6	21	0	0	16	0	0	11	71	53	6	6	32	26	89	0
Fq-h		50	39	39	30	17	22	0	0	0	9	0	4	4	13	0	43	0	4	0	0	0	11	6	22	9	4	11	6	44	0	0	0	0	0	0	17	4	0	9	39	0	0	17	56	44	6	0	30	17	83	4
Fq-i		37	16	95	47	21	16	0	5	0	0	0	0	0	0	0	16	5	0	0	0	5	5	5	42	26	16	11	5	63	5	5	0	0	0	0	11	5	0	5	37	5	5	37	79	79	37	11	37	37	74	0

SUPP MAT Figure I. Lineweaver-Burk plots for the inhibition of TcTR by a) **Nq-h** b) **Qq-b** c) **Fq-c**. The assays contained 100 μM NADPH and two fixed concentrations of inhibitor as indicated in the graph, and the TS_2 concentration was varied.

SUPP MAT Figure II. Furanquinones docked in the catalytic site of a) trypanothione reductase and b) glutathione reductase. In red, poses of higher energetic range and in yellow, lower energetic scored ranges. The preferred places are in the sourrounding of the catalytic and Z site.

SUPP MAT Figure III. Quinolinequinones docked in the catalytic site of a) trypanothione reductase and b) glutathione reductase. In red, poses of higher energetic range and in yellow, lower energetic scored ranges. The preferred places are in the sourrounding of the catalytic and Z site**.**

SUPP MAT Figure IV. The set of 28 quinones docked in the interface site of trypanothione reductase (A and B) and glutathione reductase (C and D). In red, poses with scoring energies in the higher range and in yellow, poses with energy values in the lower range.

SUPP MAT Figure V. Docking of the aryloxy-quinones on NADPH site in: a) trypanothione reductase and b) glutathione reductase.

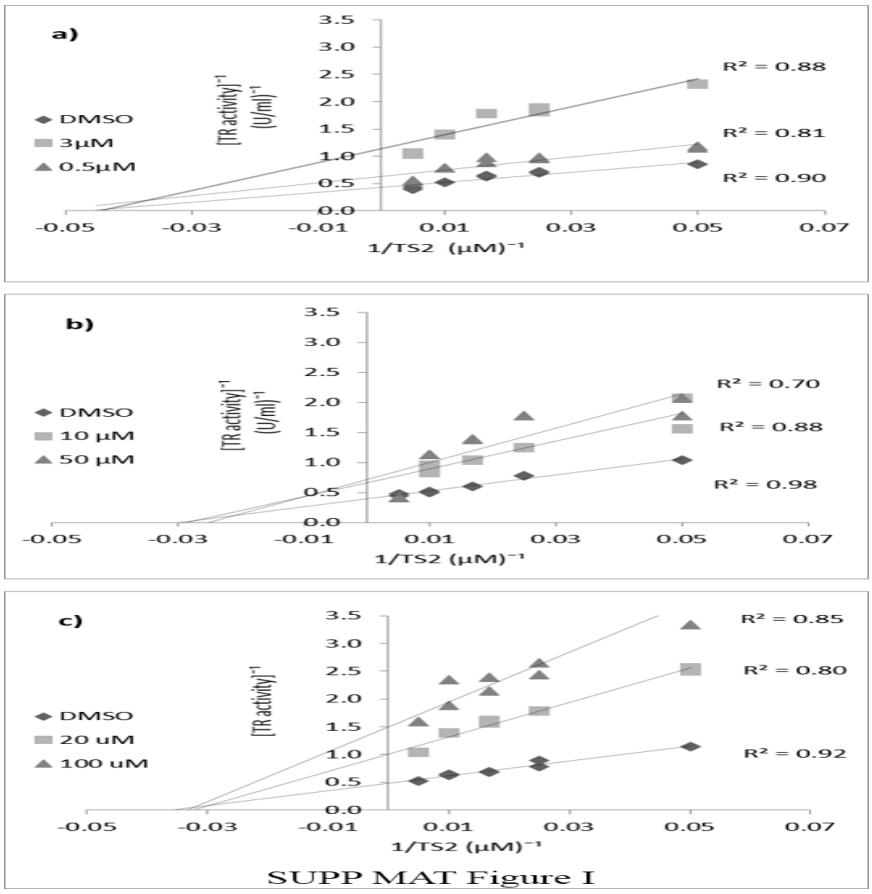

SUPP MAT Figure I

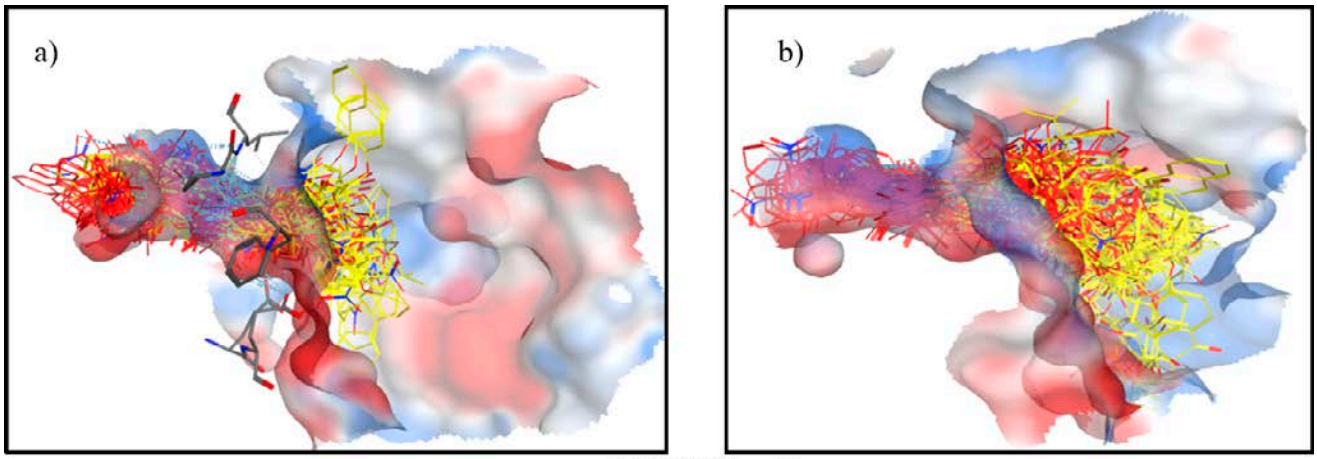

SUPP MAT Figure II

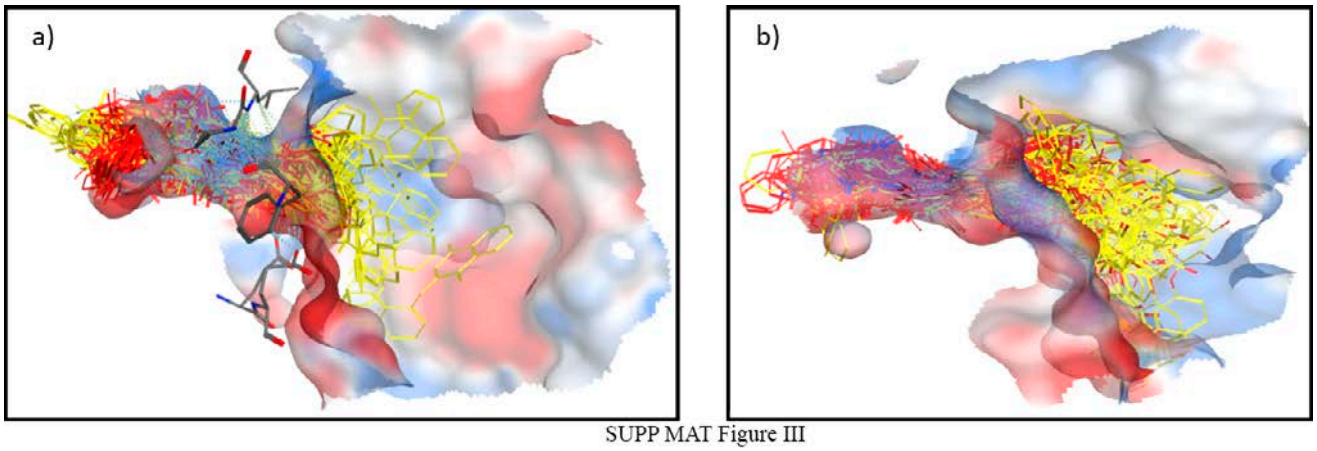

SUPP MAT Figure III

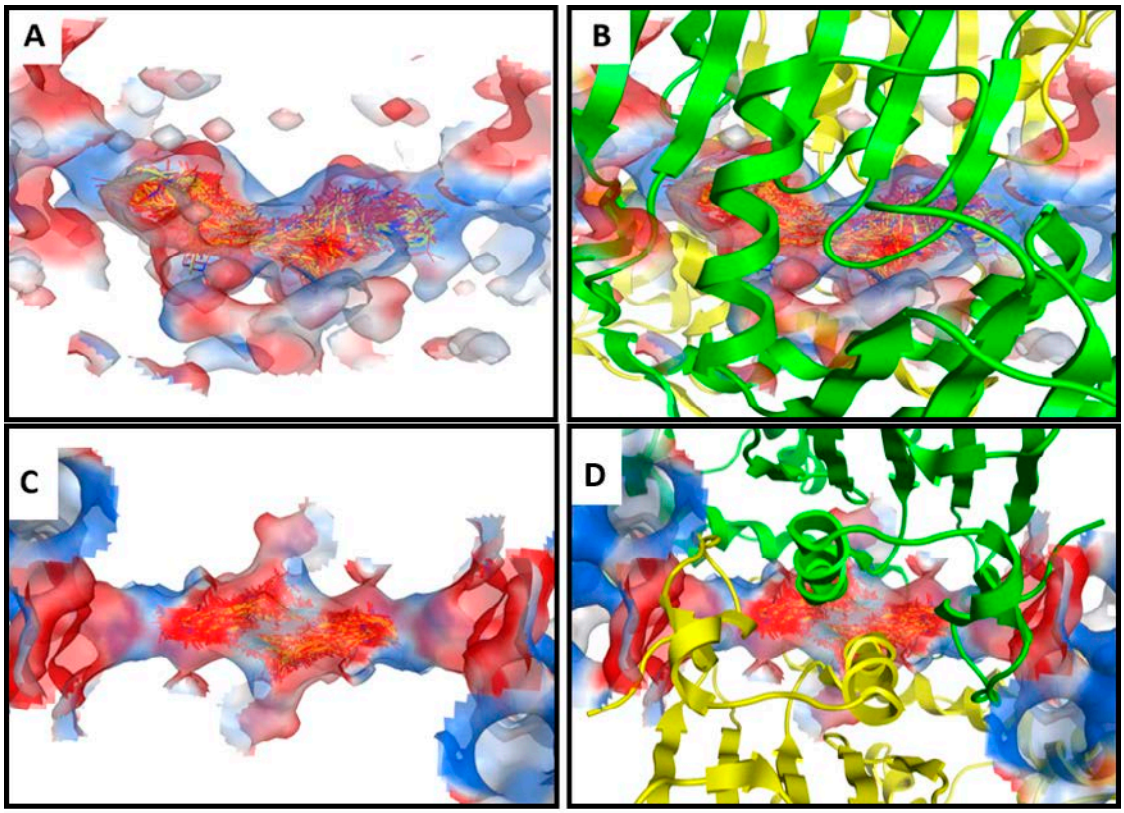

SUPP MAT Figure IV

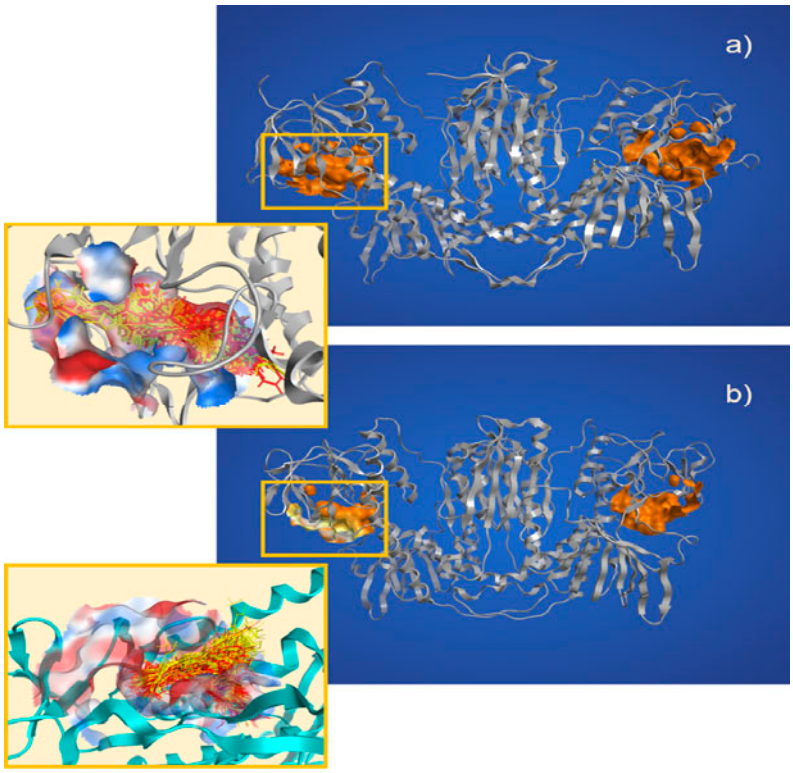

SUPP MAT Figure V

SUPPLEMENTARY MATERIAL TABLE A. Free energies of binding (ΔG) In silico in kcal/mol in trypanothione and glutathione reductases by both Q and NADPH sites.

Molecule	Trypanothione Reductase		Glutathione Reductase	
	ΔG In silico (Q site)	ΔG In silico (NADPH site)	ΔG In silico (Q site)	ΔG In silico (NADPH site)
Naphthoquinones				
Nq-a	-10.08		-10.5	
Nq-b	-11.7	-10.0	-11.1	-10.8
Nq-c	-11.6	-9.7	-11.4	-10.1
Nq-d	-11.0		-11.8	
Nq-e	-12.5	-9.7	-12.6	-11.6
Nq-f	-12.1		-11.9	
Nq-g	-12.2	-6.2	-10.9	-10.7
Nq-h	-13.4	-7	-11.6	-12.4
Nq-i	-12.1	-8.6	-11.7	-10.6
Nq-j	-9.97	-8.5	-11.2	-11.0
Furanquinones				
Fq-a	-11.1	-8.2	-12.2	-10.1
Fq-b	-12.8	-9.3	-13.1	-10.1
Fq-c	-11.3	-8.5	-12.5	-10.2
Quinolinquinones				
Qq-b	-11.7		-10.7	
Qq-c	-12.0	-9.0	-10.9	-10.8
Qq-d	-12.7	-10.0	-12.1	-10.7
Qq-e	-11.2	-10.0	-11.5	-10.7
Qq-g	-12.7	-5.2	-11.8	-9.8
Qq-i	-12.5	-9.1	-12.2	-10.3

SUPPLEMENTARY MATERIAL TABLE B. PLIF-HeatMap representing the amount (percentage) of conformers of a quinone making a contact with a given amino acid in TR or GR detected by PLIF. X-axis: aminoacid and contact codes. Y-axis: aryloxy-quinones set. Contact codes are: Side chain H-donor and acceptor (ChDon), Backbone H-donor and acceptor (BkDon), and Surface contact (Surf). Blocks are colored along a gradient from white (low percentage of contact) to dark red (high percentage of contact). Dark red blocks indicate a highly frequent contact. Black frames were used to groupe similar residues in TR/GR. The amount of conformers here represented are despicted in the TABLE 5.